© 2021. Published by The Company of Biologists Ltd | Journal of Cell Science (2021) 134, jcs259376. doi:10.1242/jcs.259376

CORRECTION

Correction: TLR7 trafficking and signaling in B cells is regulated by the MHCII-associated invariant chain

Mira Tohme, Lucie Maisonneuve, Karim Achour, Michaël Dussiot, Sophia Maschalidi and Bénédicte Manoury

There was an error in *J. Cell. Sci.* (2020) **133**, jcs236711 (doi:10.1242/jcs.236711).

The authors wish to correct an error in the 'Cells and stimulations' section of the Materials and Methods of this article, where the text incorrectly described the kit used to purify splenic B cells as a CD19-negative selection kit, instead of a CD19-positive selection kit.

The correct text is as follows:

'Splenic IgM^+/IgD^+ mature B cells were isolated using a CD19-positive selection kit [Miltenyi Biotec (130-121-301), 90–95% purity as determined by fluorescence-activated cell sorting (FACS)] and immature IgM^+/IgD^- B cells were isolated and collected by flow cytometry.'

The authors apologise to readers for this error, which does not impact the results or the conclusions of the article. Both the online full text and PDF versions of the article have been corrected.

© 2020. Published by The Company of Biologists Ltd | Journal of Cell Science (2020) 133, jcs236711. doi:10.1242/jcs.236711

RESEARCH ARTICLE

SPECIAL ISSUE: CELL BIOLOGY OF THE IMMUNE SYSTEM

TLR7 trafficking and signaling in B cells is regulated by the MHCII-associated invariant chain

Mira Tohme[1], Lucie Maisonneuve[2,3], Karim Achour[4], Michaël Dussiot[5], Sophia Maschalidi[6] and Bénédicte Manoury[2,3,*]

ABSTRACT

Toll-like receptor 7 (TLR7) is an endosomal receptor that recognizes single-stranded RNA from viruses. Its trafficking and activation is regulated by the endoplasmic reticulum (ER) chaperone UNC93B1 and lysosomal proteases. UNC93B1 also modulates major histocompatibility complex class II (MHCII) antigen presentation, and deficiency in MHCII protein diminishes TLR9 signaling. These results indicate a link between proteins that regulate both innate and adaptive responses. Here, we report that TLR7 resides in lysosomes and interacts with the MHCII-chaperone molecule, the invariant chain (Ii) or CD74, in B cells. In the absence of CD74, TLR7 displays both ER and lysosomal localization, leading to an increase in pro-inflammatory cytokine production. Furthermore, stimulation with TLR7 but not TLR9, is inefficient in boosting antigen presentation in Ii-deficient cells. In contrast, in B cells lacking TLR7 or mutated for UNC93B1, which are able to trigger TLR7 activation, antigen presentation is enhanced. This suggests that TLR7 signaling in B cells is controlled by the Ii chain.

KEY WORDS: Toll-like receptor 7, Invariant chain, B cells, UNC93B1

INTRODUCTION

Toll-like receptors (TLRs) recognize specific motifs from microbial molecules and initiate immune responses. TLRs belong to the family of single membrane-spanning receptors and are expressed in immune cells including B cells. Intracellular TLRs sense nucleic acids. Indeed, RNA or DNA from pathogen is recognized by TLR3, TLR7, TLR8 and TLR9 specifically. TLR7 senses imidazoquinoline derivatives such as imiquimod and single-stranded RNA from a wide variety of viruses such as influenza and HIV (Hemmi et al., 2002; Lund et al., 2004). Activation of intracellular TLRs by their ligands induces the recruitment of adaptor molecules, MyD88 for TLR7, TLR8 and TLR9, and TRIF (also known as TICAM1) for TLR3. Once recruited to their specific TLRs, adaptor proteins can activate two signaling pathways: the translocation of NF-κB or interferon response factor (IRF) into the nucleus for transcription of pro-inflammatory or interferon genes, respectively. The localization, traffic and folding of intracellular TLRs are regulated by the endoplasmic reticulum (ER)-resident protein UNC93B1 (Tabeta et al., 2006; Brinkmann et al., 2007; Pelka et al., 2018; Majer et al., 2019). UNC93B1 binds directly to the transmembrane region of TLR3, TLR7, TLR8 and TLR9 in the ER and transports them to endocytic compartments upon stimulation (Kim et al., 2008). In dendritic cells (DCs) purified from mice expressing a point mutation in UNC93B1 (3d), intracellular TLRs are retained in the ER, preventing DCs from secreting cytokines upon engagement of TLR3, TLR7 and TLR9 (Tabeta et al., 2006). However, in B cells, even though UNC93B1 is still required for intracellular TLR signaling, TLR9 seems, at the steady state, to reside in lysosomal compartments (Avalos et al., 2013). In addition, mice or humans deficient for UNC93B1 are susceptible to multiple infections (Tabeta et al., 2006; Casrouge et al., 2006; Melo et al., 2010; Caetano et al., 2011). Intracellular TLRs require proteolytic cleavage in acidic endosomes for their activity (Park et al., 2008; Matsumoto et al., 2008; Ewald et al., 2008; Sepulveda et al., 2009). Indeed, cells from different origins and deficient for asparagine endopeptidase (AEP) show significant decrease in cytokine production following TLR7 stimulation with imiquimod or infection with influenza virus (Maschalidi et al., 2012). Also, inhibition of furin-like proprotein convertases severely diminishes TLR7 signaling (Hipp et al., 2013).

B cells are dedicated cells in adaptive immunity as they present exogenous antigen on major histocompatibility complex class II (MHCII) molecules to $CD4^+$ T cells. MHCII α and β chains assemble and form heterodimers in the ER, where they associate with a chaperone molecule, the invariant chain (Ii) or CD74 (Roche et al., 1991). A prerequisite for peptide loading onto MHCII molecules is the proteolytic destruction of Ii. The N-terminal cytoplasmic domain of Ii targets the MHCII–Ii complexes to the endocytic pathway (Zhong et al., 1997). Ii is sequentially cleaved, leaving a C-terminal portion: the class II invariant chain peptide or CLIP, which protects the class II peptide binding groove from binding peptides outside the endocytic compartments. In lysosomal vesicles, the chaperone molecule DM interacts with the complex MHCII–CLIP and facilitates the exchange of CLIP for peptides generated in the endocytic pathway (Denzin and Cresswell, 1995). Thus, Ii chains plays a critical role in MHCII antigen presentation to $CD4^+$ T cells by stabilising MHCII in the ER and directing MHCII to endocytic compartments. Ii also interacts with MHCI and promotes antigen cross-presentation by DCs (Basha et al., 2012). In addition to their classical functions in antigen presentation, a recent study has shown that MHCII molecules are important components in the TLR response (Liu et al., 2011). MHCII deficiency in DCs and macrophages lowers the secretion of pro-inflammatory cytokines and type I interferon following TLR3, TLR4 or TLR9 stimulation. MHCII forms a complex with the activated Bruton's tyrosine kinase (Btk) induced by TLR stimulation, allowing a

[1]Nkarta Therapeutics, South San Fransisco, CA 94080, USA. [2]Institut Necker Enfant Malade, INSERM U1151-CNRS UMR 8253, 75015 Paris, France. [3]Université de Paris, Faculté de médecine, 75015 Paris, France. [4]Institut de recherche Servier, 3 rue de la république, 92150 Suresnes, France. [5]Institut Imagine, INSERM U1163, CNRS ERL 8254, Université Paris Descartes, Sorbonne Paris-Cité, Laboratoire d'Excellence GR-Ex, 75015 Paris, France. [6]VIB-UGent Center for Inflammation Research, UGent-VIB Research Building FSVM, Technologiepark 71, 9052 Ghent, Belgium.

*Author for correspondence (benedicte.manoury@inserm.fr)

B.M., 0000-0001-7784-3389

Received 19 July 2019; Accepted 4 February 2020

Journal of Cell Science (2020) 133, jcs236711. doi:10.1242/jcs.236711

sustained interaction with MyD88 and activation of the NF-κB and IRF pathways.

Because Ii chain is a key chaperone in MHCII trafficking and folding, we investigated the role of CD74 in regulating TLR7 and TLR9 responses. Here, we show that CD74 interacts with TLR7 expressed in lysosomes and modulates specifically TLR7 but not TLR9 response in B cells. In B cells lacking CD74, stimulation of TLR7 initiates cytokine production and inhibits antigen presentation, whereas in B cells lacking TLR7 or mutated for UNC93B1, antigen presentation is increased. These results suggest that Ii chain in B cells dampens TLR7 innate immune responses to promote adaptive immunity.

RESULTS

Absence of Ii expression promotes TLR7 signaling in B cells

To assess whether Ii plays a role in TLR signaling, we stimulated membrane and intracellular TLRs from wild type (wt) ($Ii^{+/+}$) and Ii-deficient ($Ii^{-/-}$) bone marrow-derived dendritic cells (BMDCs), macrophages (BMDMs) and B cells with TLR-specific ligands. Ii-deficient B cells produced significantly more interleukin 6 (IL-6) and tumor necrosis alpha (TNF-α) than wt B cells in response to two TLR7 ligands: imiquimod and gardiquimod (Fig. 1A; Fig. S1A). In contrast, $Ii^{-/-}$ B cells responded normally to TLR9 and TLR4 stimulation and produced similar amounts of IL-6 and TNF-α to those produced by $Ii^{+/+}$ B cells (Fig. 1A; Fig. S1A). No difference in TLR7 mRNA or protein expression was detected between $Ii^{+/+}$ and $Ii^{-/-}$ B cells (Fig. S1B,C). In addition, CD69, an activation marker expressed by B cells, was upregulated in Ii-deficient B cells upon TLR7, but not TLR9, stimulation (Fig. 1B) in comparison to wt cells. Surprisingly, no difference in cytokines secretion was observed when wt BMDCs or BMDCs lacking Ii chain were stimulated with TLR4, TLR7 or TLR9 ligands (Fig. S1D). Similar results were obtained with BMDMs (Fig. S1E). TLR7 stimulation induces the recruitment of the adaptor protein MyD88 followed by the translocation of the transcription factor NF-κB into the nucleus leading to the production of pro-inflammatory cytokines. Thus, increased TLR7 signaling correlates with stronger activation of the transcription factor NF-κB. To investigate whether or not the increase in TLR7 signaling in $Ii^{-/-}$ B cells resulted in enhanced proximity/interaction between the adaptor protein MyD88 and NF-κB, we used an *in situ* proximity-ligation assay (PLA) method that gives a signal if two different molecules are localized within 40 nm of each other. This method has been widely used to monitor spatial proximity of two proteins at the subcellular level and potentially would allow us to detect and visualize MyD88 conjugated to NF-κB (Yamazaki et al., 2009; Leuchowius et al., 2011; Misawa et al., 2013; Babdor et al., 2017). First, to validate this method, we monitored interaction signals between Ii and MHCII detected as red dots by confocal microscopy. As expected, we found spatial proximity of Ii with MHCII (Fig. S2A), which was significantly reduced in the absence of Ii. We then investigated interaction and proximity signals between MyD88 and NF-κB. In $Ii^{+/+}$ B cells, interaction signals between endogenous MyD88 and NF-κB were detected when cells were stimulated with imiquimod (Fig. 1C) and were significantly increased in $Ii^{-/-}$ B cells. Furthermore, no signal was observed in unstimulated cells (Fig. 1C). As expected, similar interaction signals between MyD88 and NF-κB were observed in TLR7-stimulated $Ii^{+/+}$ and $Ii^{-/-}$ BMDCs (Fig. S2B).

It was reported by the group of Cao that MHCII molecules promote full activation of TLR3, TLR4 and TLR9 in macrophages and DCs by interacting with CD40 and Btk to prolong Btk phosphorylation needed for TLR activation (Liu et al., 2011). Thus, we investigated whether MHCII was also required for TLR7 function in B cells. We then stimulated wt ($MHCII^{+/+}$) and MHCII-deficient ($MHC\text{-}II^{-/-}$) B cells with different TLR agonists. We observed no substantial difference in cytokine production between $MHCII^{+/+}$ and $MHCII^{-/-}$ B cells when TLR4, TLR7 or TLR9 were activated (Fig. S2C). Accordingly, expression of Btk or CD40 was the same in $Ii^{+/+}$ and $Ii^{-/-}$ resting and TLR7-stimulated B cells (Fig. S2D).

Recognition of the B-cell receptor (BCR) by antigen triggers BCR signaling and endocytosis. CpG-DNA- and BCR-induced TLR9 and antigen signaling have been shown to synergize in NF-κB induction and p38 phosphorylation (Chaturvedi et al., 2008). Thus, we treated wt and Ii-deficient B cells with imiquimod to stimulate TLR7 or with Fab-anti-mouse IgM together with imiquimod to engage both BCR and TLR7 and monitored cytokine production. As expected, dual stimulation through BCR and TLR7 increased IL-6 and TNFα production in wt B cells in comparison to TLR7 activation alone. This response was further amplified in Ii-deficient B cells but not in $MHCII^{-/-}$ B cells (Fig. 1D). Ii deficiency was shown to alter B cell maturation. Therefore, to exclude the hypothesis that the increased in TLR7 response detected in B cells lacking Ii was a result of a lack of B cell maturation, immature B cells were purified from bone marrow and TLRs were stimulated. Overall, wt immature B cells were unresponsive to TLR activation. However, similarly to mature B cells, $Ii^{-/-}$ immature B cells produced more IL-6 and TNF-α in response to TLR7 but not to TLR9 and TLR4 stimulation (Fig. S3).

Ii chain interacts with TLR7 upon stimulation

The results described above indicate that Ii might be part of the TLR7 signaling pathway. To address this, complementary DNA (cDNA) coding for hemagglutinin (HA)-tagged full-length TLR7 and wt Ii were co-transfected in fibroblast. Forty-eight hours later, TLR7–Ii complexes were immunoprecipitated with an HA-conjugated antibody and blotted for Ii expression. As shown in Fig. 2A, Ii interacts with TLR7 upon imiquimod stimulation. However, to look at possible Ii–TLR7–MyD88 proximity/interactions in B cells, we used the DuoLink *in situ* PLA method described above because specific antibodies for detecting endogenous TLR7 working in immunofluorescence or immunoprecipitation were unavailable. We transfected a cDNA coding for HA-tagged full-length TLR7 in B cells and monitored the interaction of the transfected TLR7 protein with endogenous Ii. In a wt mouse B cell line (II.A1.6), interaction signals between endogenous Ii chain and transfected TLR7 were detected only when cells were stimulated with imiquimod (Fig. 2B). To investigate whether this interaction was specific for Ii chain, we used short hairpin RNA (shRNA) lentiviral particles targeting the Ii chain to silence Ii chain expression. Ii chain knockdown was confirmed using the individual shRNA 89 construct targeting a specific region of Ii and visualized by western blotting (Fig. 2C). The lower expression of Ii chain resulted in a significant decrease in the interaction signal between TLR7 and Ii previously observed upon TLR7 stimulation (Fig. 2B,C). Interestingly, the peak of interaction between Ii chain and TLR7 was observed after 30 min of imiquimod incubation (Fig. 2B, right panel). Upon imiquimod sensing, TLR7 associates with MyD88 to allow signal transduction (Ewald et al., 2008; Maschalidi et al., 2012). Therefore, we performed similar experiments as described above to visualize the proximity signal between Ii chain and MyD88. Upon TLR7 engagement, positive PLA signals corresponding to proximity between Ii and MyD88 were present in the cells (Fig. 2D, left). Again the maximum signal was visualized after

Journal of Cell Science (2020) 133, jcs236711. doi:10.1242/jcs.236711

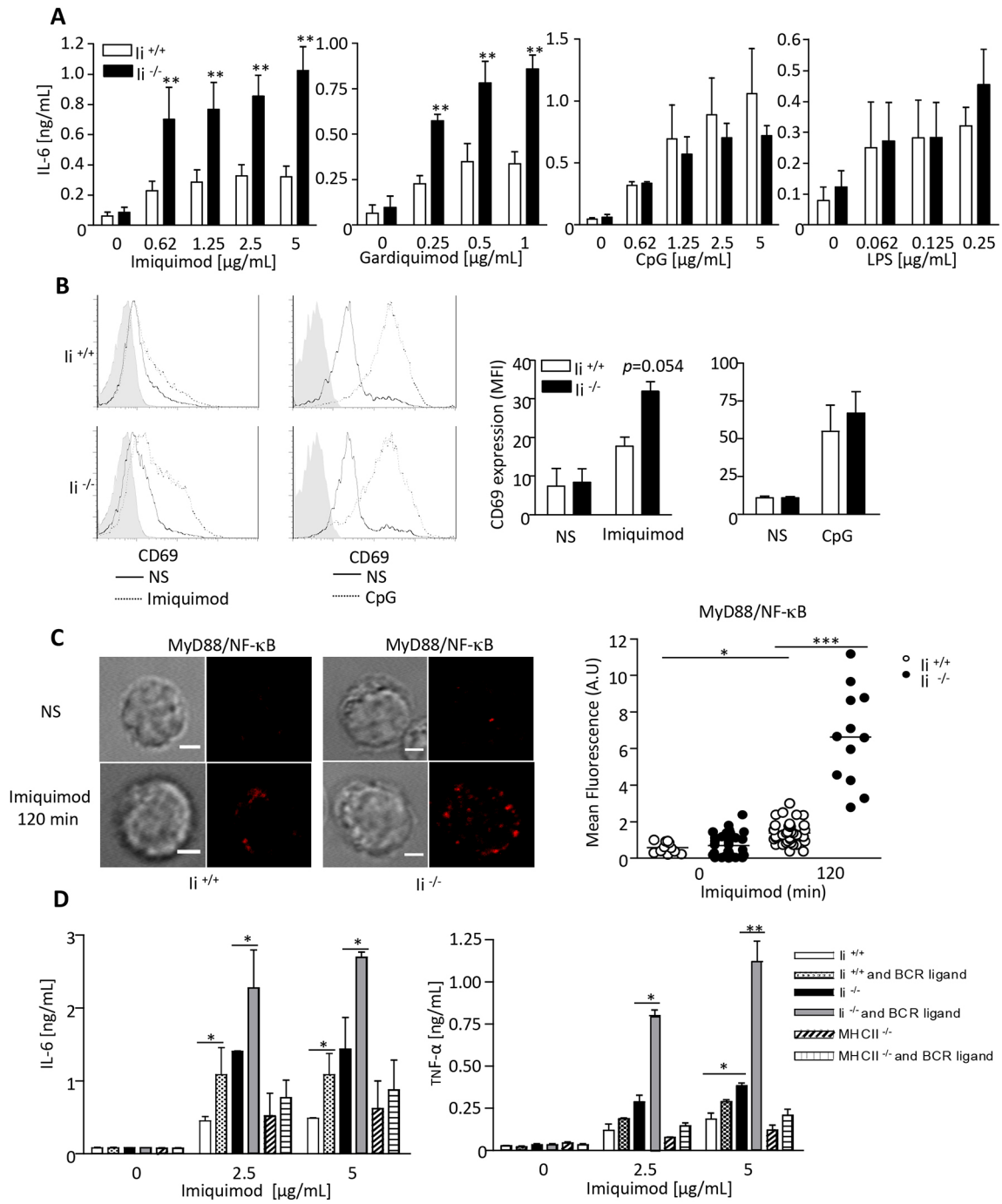

Fig. 1. TLR7-specific stimulation increases IL-6 production, CD69 expression and Myd88–NF-κB interaction in Ii-deficient B cells. (A) Ii$^{+/+}$ or Ii$^{-/-}$ mature splenic B cells were stimulated with different TLR ligands for 12 h and secretion of IL-6 was measured by ELISA (n=8, graphs show mean±s.e.m., **P<0.01). (B) Mouse splenic B cells were treated without (black lines) or with (dashed lines) 5 µg/ml imiquimod or 10 µg/ml CpGB for 16 h and stained for CD69 expression using fluorescent antibodies. Gray histograms represent staining of B cells with the antibody isotype control. Quantification of three experiments using Prism is shown on the right. (C) Detection of Myd88 and NF-κB interaction using the proximity ligation assay (PLA) *in situ* in Ii$^{+/+}$ and Ii$^{-/-}$ mature splenic B cells unstimulated (NS) or stimulated with imiquimod for 120 min. PLA signals are shown in red. One representative experiment out of three is shown. Quantification of mean fluorescence using ImageJ software is shown on the right (n=12–30 cells, *P<0.05, ***P<0.001). (D) IL-6 and TNF-α production in supernatants from Ii$^{+/+}$, Ii$^{-/-}$, MHCII $^{+/+}$ or MHCII$^{-/-}$ mature B cells stimulated with imiquimod alone or together with BCR ligand (n=3, graphs show mean±s.e.m., *P<0.05). Scale bars: 5 µm.

30 min of TLR7 engagement (Fig. 2D, right). To confirm that this interaction involved TLR7, Ii–MyD88 association in primary mouse B cells was monitored in the absence of TLR7. Indeed, no association between Ii chain and the adaptor protein MyD88 was observed in TLR7$^{-/-}$ B cells in comparison to TLR7$^{+/+}$ cells (Fig. 2E). In contrast, we did not observe any interaction between TLR9 and Ii chain in B cells when TLR9 was stimulated (Fig. 2F). In conclusion, Ii chain specifically associates with TLR7 and its adaptor molecule MyD88 but not with TLR9 in B cells.

Journal of Cell Science (2020) 133, jcs236711. doi:10.1242/jcs.236711

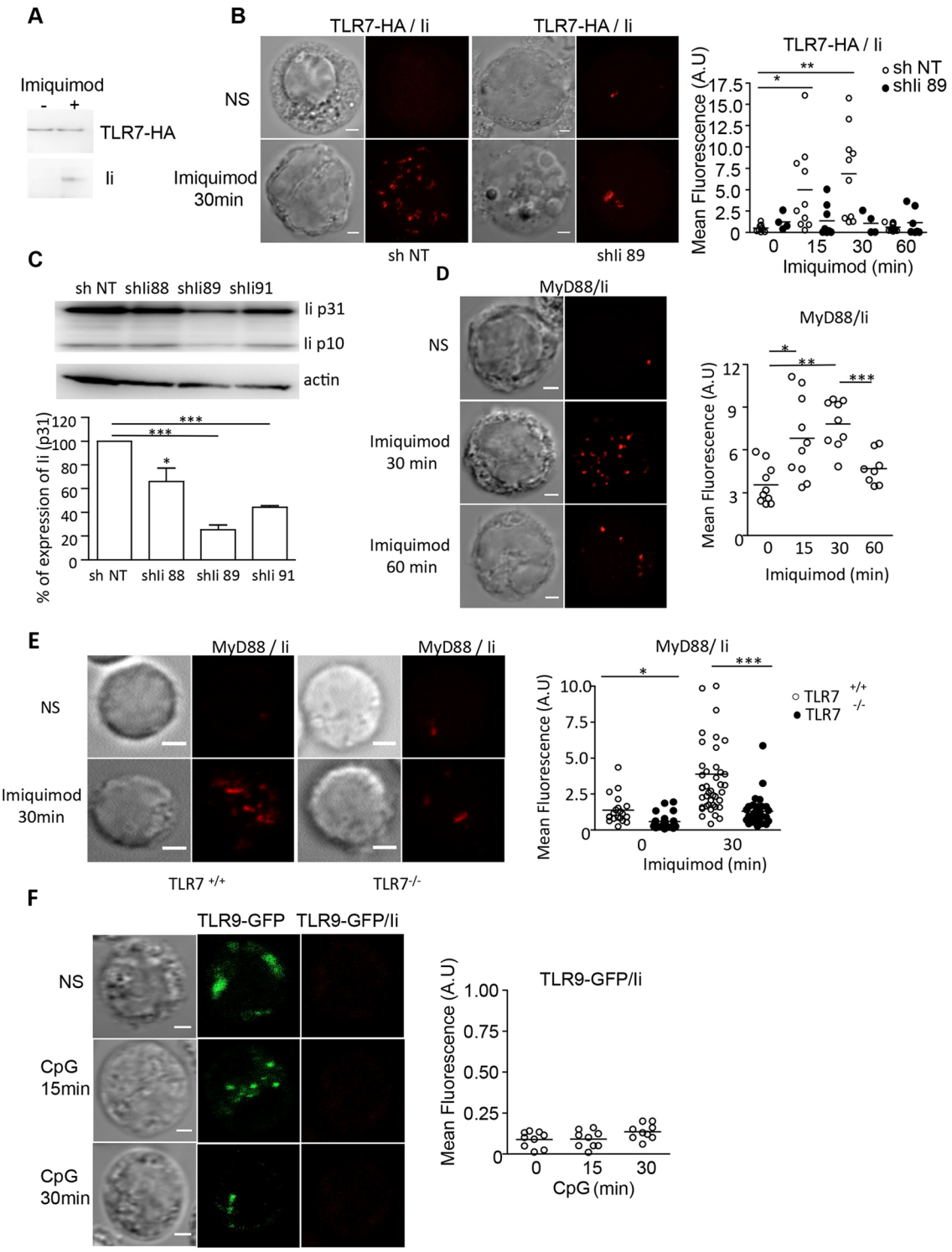

Fig. 2. Ii interacts with or is in proximity to TLR7 and the adaptor molecule MyD88. (A) Fibroblasts were stimulated with imiquimod (5 µg/ml) for 30 min. TLR7 was immunoprecipitated from lysates and TLR7 and Ii expression was analyzed by western blot. One representative experiment out of three is shown. (B) Detection of Ii and TLR7 interaction using PLA *in situ* with anti-HA and anti-Ii specific mAbs in IIA1.6 B cell line infected with lentiviruses carrying a shRNA sequence for Ii or a shRNA sequence control (ShNT). Cells were stimulated or not (NS) with imiquimod for different times. PLA positive signals are shown in red. One representative experiment out of three is shown. Quantification of mean fluorescence using ImageJ software (n=10 cells, *P<0.05, **P<0.01). (C) Anti-Ii and β-actin immunoblot of the B cell line IIA1.6 line infected with lentiviruses carrying different shRNA sequences for Ii or shRNA sequence control (ShNT). Quantification of three experiments using ImageJ software is shown below (n=3, *P<0.05, ***P<0.001). Detection of MyD88 and Ii interaction using PLA *in situ* with anti-MyD88 and anti-Ii specific mAbs in IIA1.6 B cell line (D) or in TLR7$^{+/+}$ or TLR7$^{-/-}$ primary B cells (E) following imiquimod stimulation for different times. One representative experiment out of three is shown. Quantification of mean fluorescence using ImageJ is shown on the right of each panel (n=10 cells for C and n=30 cells for D, *P<0.05, **P<0.01 ***P<0.001). (F) Detection of Ii and TLR9 interaction using PLA *in situ* with anti GFP and anti-Ii specific mAbs in resting and CpG-stimulated primary B cells for different times, left panel. Quantification of mean fluorescence using ImageJ is shown on the right (n=10 cells). Lines in scatter plots indicate mean values. Scale bars: 5 µm.

Journal of Cell Science (2020) 133, jcs236711. doi:10.1242/jcs.236711

Ii chain regulates TLR7 trafficking in B cells

To determine where TLR7 is localized in $Ii^{+/+}$ B cells and whether or not Ii chain influences TLR7 trafficking, we first assessed by confocal microscopy the subcellular distribution of HA-tagged TLR7 construct in resting and activating $Ii^{+/+}$ and $Ii^{-/-}$ B cells. Transfection efficiency of the HA-tagged TLR7 construct was the same in $Ii^{+/+}$ and $Ii^{-/-}$ B cells (~30%; Fig. S4). Ii acts as a chaperone for MHCII folding, transport and antigen presentation, and thus, in the absence of Ii, MHCII might accumulate in ER-related structures (Viville et al., 1993). Thus, to investigate the integrity of lysosomes in Ii-deficient B cells, we incubate B cells with the Lysotracker dye, which stains lysosomes. Similar lysosomal fluorescence was detected in both $Ii^{+/+}$ and $Ii^{-/-}$ B cells expressing either TLR7 or TLR9 (Fig. 3A,B). Using confocal microscopy in TLR7-HA-expressing B cells, TLR7 staining was observed in small intracellular vesicles that contained the accessory protein H2-DM, Ii chain and MHCII molecules (Fig. 4A; Fig. S5A) both at steady state and upon TLR7 stimulation. These intracellular vesicles correspond to lysosomes as they stain positive for the lysosomal marker LAMP-1 (Fig. S6A). Additional experiments indicated that TLR7 did not reside in the ER, the ER-Golgi intermediate compartment or in early endosomes, as shown by the absence of TLR7 localization in calreticulin-, TAP1-, ERGIC53 (also known as LMAN1)- or VAMP3-positive compartments (Fig. S6B,C). In contrast, in resting or activated $Ii^{-/-}$ B cells, TLR7 was localized in ER vesicles that stained positive for calreticulin and less in the ER-Golgi intermediate compartment positive for ERGIC53 or in small intracellular vesicles containing VAMP3, H2-DM, Ii chain and MHCII molecules (Fig. 4A; Figs S5A and S6B,C). Quantification showed that the difference in TLR7-HA localization between $Ii^{-/-}$ and $Ii^{+/+}$ B cells is highly significant (Fig. 4A, bottom panel). Next, we monitored endogenous TLR7 localization using imaging flow cytometry. In resting or activated $Ii^{-/-}$ B cells, TLR7 levels were higher in ER vesicles that stained positive for calnexin in comparison to $Ii^{+/+}$ B cells (Fig. 4B; Fig. S5B). However, TLR7 was also detected in LAMP-1-positive lysosomal organelles, although significantly less than in $Ii^{+/+}$ B cells (Fig. 4B). In addition, cross-linking the BCR with anti-IgM along with imiquimod treatment did not change the localization of TLR7 (Fig. 5A) in Ii-deficient B cells. Like TLR7, at steady state and upon CpG stimulation with or without BCR cross-linking, TLR9 also resides in lysosomal compartments and not in the ER, as it colocalizes with MHCII and H2-DM but not with calreticulin marker (Fig. 5B; Fig. S7A,B).

Altogether, these results demonstrate that TLR7 and TLR9, unlike in DCs, reside in lysosomal compartments in B cells at steady state after intracellular TLR stimulation, and that Ii regulates TLR7 trafficking in B cells.

TLR7 subcellular localization is independent of UNC93B1

UNC93B1 is a chaperone molecule for endosomal TLRs (Tabeta et al., 2006; Pelka et al., 2018). It associates with intracellular TLRs resident in the ER and mediates their translocation to endosomal or lysosomal compartments (Kim et al., 2008; Majer et al., 2019). Surprisingly, we observed that TLR9, unlike TLR7, partially colocalized with UNC93B1 when cells were activated or not with CpG or imiquimod (Fig. 6A). UNC93B1 and Ii staining seems to

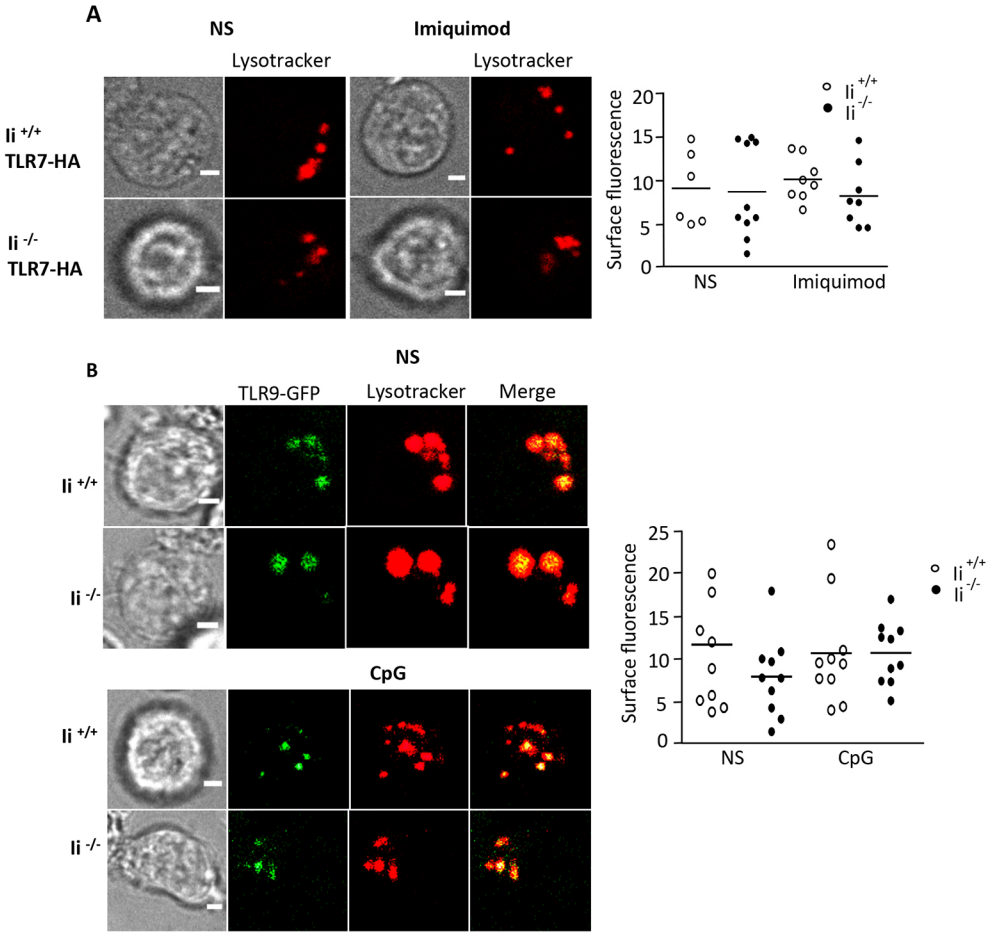

Fig. 3. Lysosome integrity is intact in Ii-deficient B cells. Immunofluorescence microscopy of resting or TLR-stimulated $Ii^{+/+}$ and $Ii^{-/-}$ splenic B cells transfected with full-length (FL)-TLR7-tagged HA (A) or with FL-TLR9-tagged GFP (B) and immunostained for TLR9 (green) and lysosomes (red) using Lysotracker dye. Images shown are taken 30 min after incubation with the Lysotracker. One experiment representative of three is shown. Graphs on the right in A and B show quantification of fluorescence intensity using ImageJ software (n=6–10 cells). Lines in scatter plots indicate mean values. Scale bars: 5 µm.

Journal of Cell Science (2020) 133, jcs236711. doi:10.1242/jcs.236711

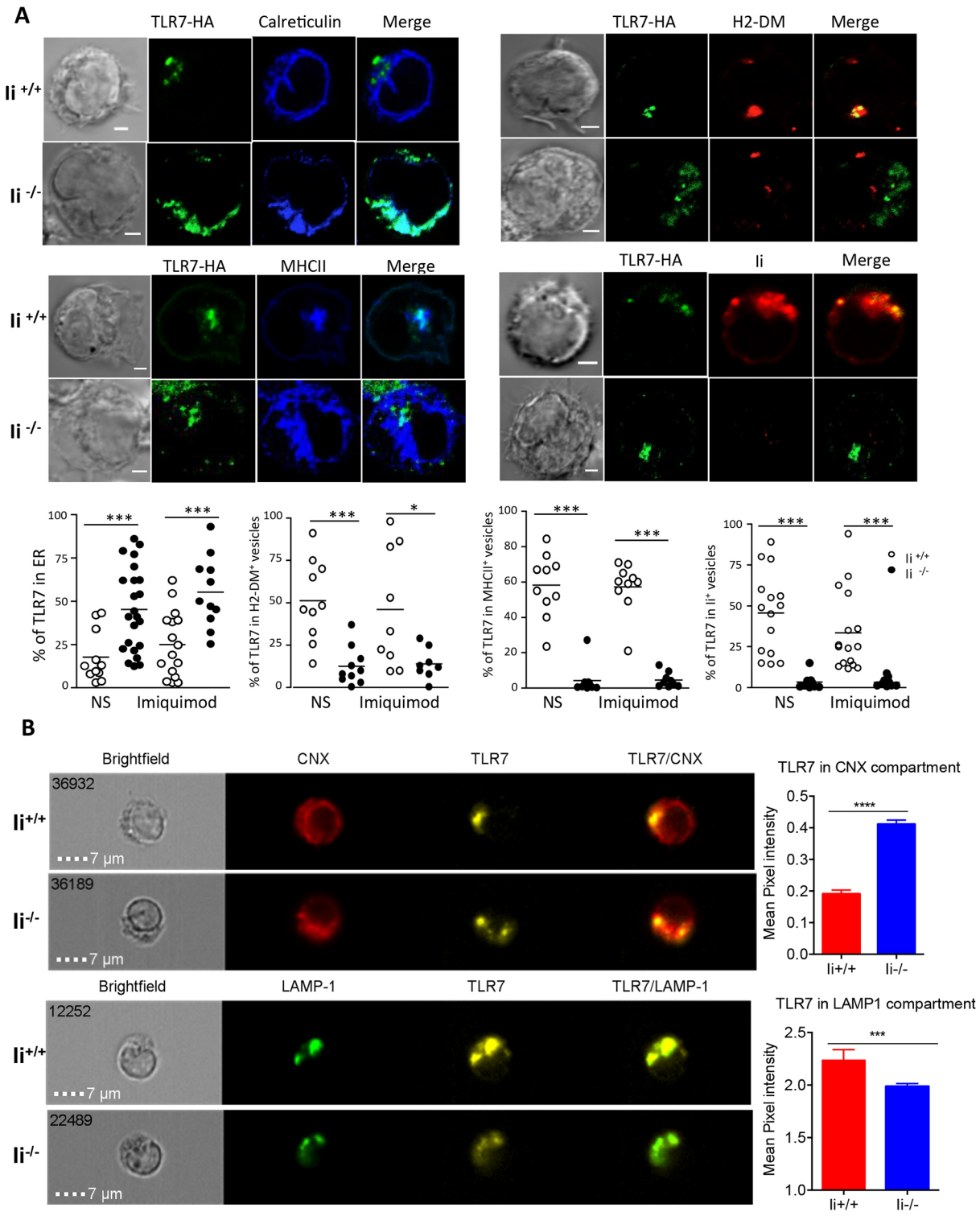

Fig. 4. Ii regulates TLR7 trafficking in B cells. (A) Immunofluorescence microscopy of resting $Ii^{+/+}$ or $Ii^{-/-}$ splenic B cells transfected with FL-TLR7-tagged HA and immunostained for TLR7 (green), calreticulin (blue), H2-DM (red), MHCII (blue) and Ii (red). One experiment representative of three is shown. Quantification of colocalization using ImageJ is shown in graphs below (n=10 cells, *P<0.05, ***P<0.001). (B) Representative images of calnexin (CNX), LAMP-1 and TLR7 intracellular staining in resting B cells from $Ii^{+/+}$ or $Ii^{-/-}$ acquired by imaging flow cytometry. First column shows cells in brightfield, second column ER or lysosomal markers (CNX or LAMP-1), third column TLR7, fourth column merged. Graphs show quantification of colocalization (mean pixel intensity±s.e.m.; CNX-TLR7: $Ii^{+/+}$, 0.1905±0.012, n=5045 and $Ii^{-/-}$, 0.4110±0.0013, n=6478; LAMP-1-TLR7: $Ii^{+/+}$, 2.236±0.1017, n=1328 and $Ii^{-/-}$, 1.987±0.0278, n=6213; ***P<0.001, ****P<0.0001). One experiment of three is shown. Lines in scatter plots indicate mean values. Scale bars: 5 µm.

overlap, indicating that UNC93B1 might also be localized in lysosomal vesicles in B cells (Fig. 6B). This result is strengthened by experiments using imaging flow cytometry, which showed weak colocalization of TLR7 and UNC93B1 in $Ii^{-/-}$ B cells, suggesting again, ER localization for TLR7 in B cells deficient in Ii (Fig. 6C).

Journal of Cell Science (2020) 133, jcs236711. doi:10.1242/jcs.236711

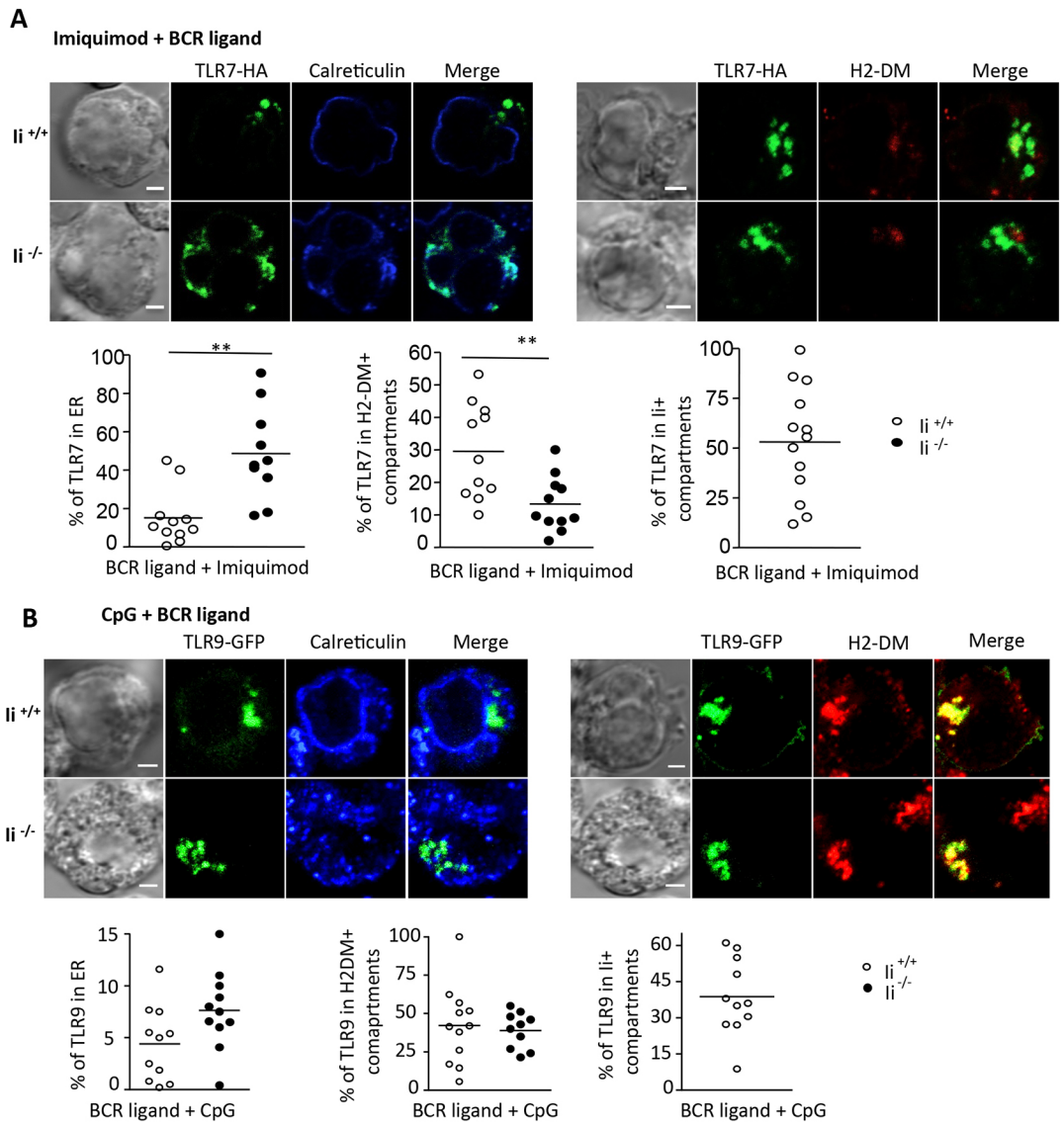

Fig. 5. BCR cross-linking does not affect TLR7 or TLR9 localization in B cells. Immunofluorescence microscopy of TLR7 or TLR9- and BCR-stimulated $Ii^{+/+}$, $Ii^{-/-}$ splenic B cells transfected with FL-TLR7-tagged HA (A) or FL-TLR9-tagged GFP (B) and immunostained for TLR7 or TLR9 (green), calreticulin (blue) and H2-DM (red). One experiment representative of three is shown. Quantification of colocalization using ImageJ (n=10–13 cells, $^{**}P$<0.01) is shown in lower panels of A and B. Lines in scatter plots indicate mean values. Scale bars: 5 µm.

The innate, but not the adaptive, function of TLR7 is exacerbated in the absence of Ii

In the absence of Ii, MHCII antigen presentation is abolished (Teyton and Peterson, 1992). So, to test the possibility that the lack of Ii regulates the balance between innate and adaptive TLR7-dependent response in B cells, as described above, in promoting cytokine production upon TLR7 sensing, we chose to assess MHC class I antigen cross-presentation. Indeed, B lymphocytes are able to cross-present exogenous antigens when they are internalized via their BCR, and MHCI cross-presentation was shown to be further enhanced when the antigen is coupled to TLR9 ligand (Heit et al., 2004; Ke and Kapp, 1996; Jiang et al., 2011). First, we assessed whether MHCI antigen cross-presentation was increased in the presence of TLR ligands. $Ii^{+/+}$, $Ii^{-/-}$ and $TLR7^{-/-}$ B cells were stimulated with soluble ovalbumin with or without imiquimod, CpG or lipopolysaccharide (LPS) for 12 h. Then, B cells were washed and incubated with carboxyfluorescein succinimidyl ester (CFSE)-labeled T cells specific for ovalbumin (OT-I cells). Three days later, T-cell proliferation was analyzed. In wt, Ii- and TLR7-deficient B cells, ovalbumin antigenic presentation led to a weak proliferation of T cells (Fig. 7A, gray histograms). However, T-cell stimulation was increased in wt B cells incubated with both ovalbumin and LPS or CpG or imiquimod (Fig. 7A, black lines). As expected, similar proliferation of OTI T cells was observed in $TLR7^{-/-}$ B cells activated with ovalbumin in the presence or absence of imiquimod, demonstrating that TLR7 stimulation specifically increases MHCI antigen cross-presentation in wt cells (Fig. 7A, bottom row). Surprisingly, the boost in T-cell proliferation observed when wt cells were stimulated with imiquimod was abolished in $Ii^{-/-}$ B cells and to a similar extent as in TLR7-deficient cells (Fig. 7A, black lines, middle row, quantification in Fig. 7B). In contrast, no difference was detected between CpG- or LPS-stimulated $Ii^{+/+}$ and $Ii^{-/-}$ cells. In addition, two concentrations of OVA-control peptide triggered similar proliferation in all cell types tested (Fig. 7C). These results suggest that TLR stimulation increases MHCI antigen cross-presentation in B cells, and that Ii chain promotes TLR7-dependent

Journal of Cell Science (2020) 133, jcs236711. doi:10.1242/jcs.236711

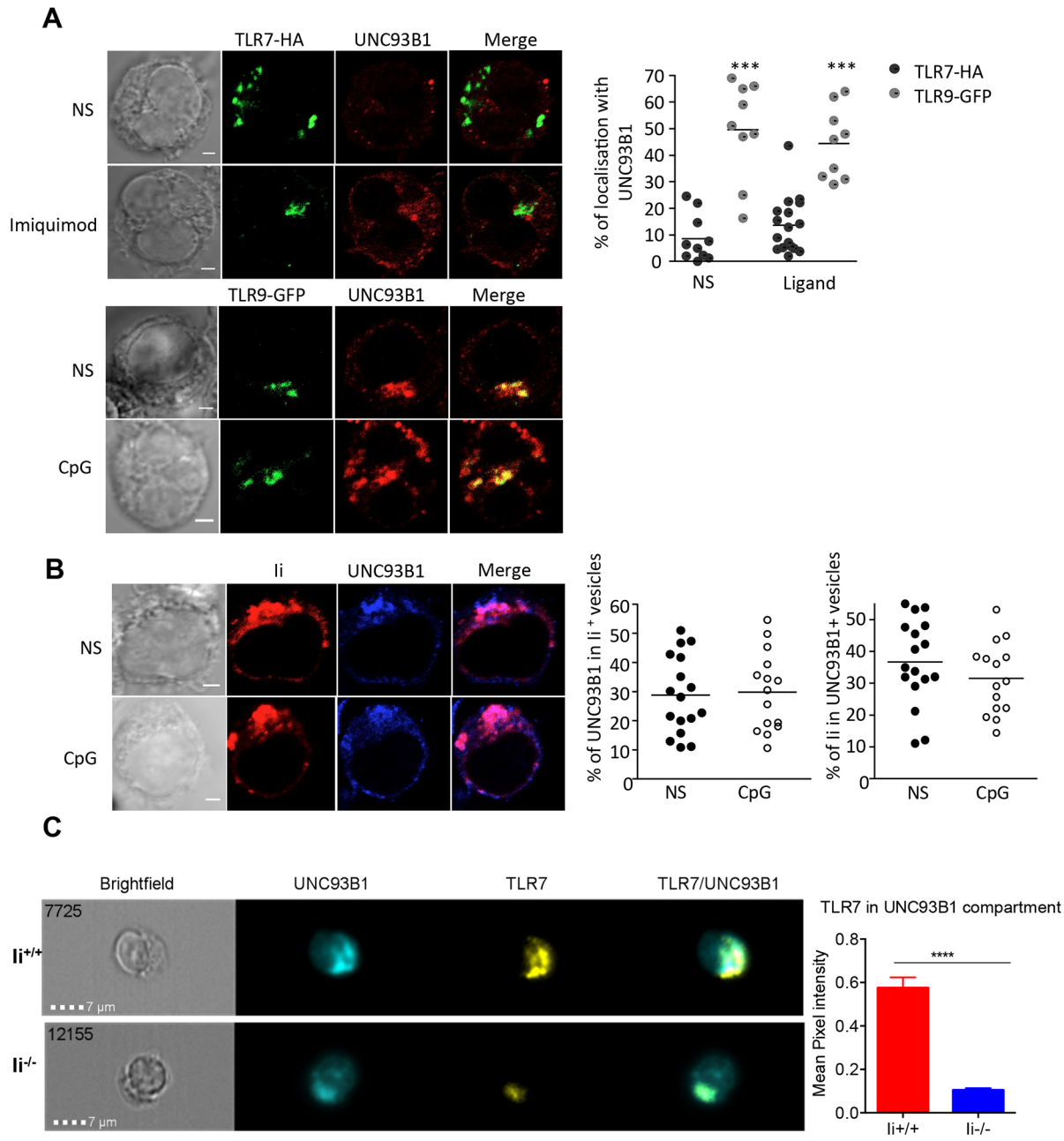

Fig. 6. TLR9, but not TLR7, colocalizes with UNC93B1. (A) Immunofluorescence microscopy of resting (NS) or TLR-stimulated splenic B cells transfected with FL-TLR7-tagged HA (top) or FL-TLR9-tagged GFP (bottom) and immunostained for TLR7 or TLR9 (green) and UNC93B1 (red). One experiment representative of three is shown. Quantification of colocalization using ImageJ is shown to the right (n=10 cells, ***P<0.001). (B) Immunofluorescence microscopy of resting (NS) or TLR9-stimulated splenic B cells immunostained for Ii (red) and UNC93B1 (blue). One experiment representative of three is shown. Quantification of colocalization using ImageJ is on the right (n=15–17 cells). (C) Representative images of UNC93B1 and TLR7 intracellular staining in resting B cells from $Ii^{+/+}$ or $Ii^{-/-}$ acquired by imaging flow cytometry. Graphs show quantification of colocalization of UNC93B1 and TLR7 (mean pixel intensity ±s.e.m. $Ii^{+/+}$, 0.5752±0.048, n=1294 and $Ii^{-/-}$, 0.1043±0.0092, n=4411; ****P<0.0001). Lines in scatter plots indicate mean values. Scale bars: 5 µm.

adaptive but not innate function in B cells. Many laboratories have described the important role of UNC93B1 in TLR trafficking, signaling, and MHCI and MHCII antigen-presentation pathways (Tabeta et al., 2006; Maschalidi et al., 2017). We then wondered whether UNC93B1 might play a similar role to Ii chain in regulating the innate and adaptive function in B cells. To address the contribution of UNC93B1 in the adaptive response in B cells, wt and UNC93B1 mutated (3d) B cells, which harbor a mutation in the transmembrane domain of UNC93B1 and inhibit intracellular TLRs signaling, were incubated with beads coated with myelin oligodendrocyte (MOG) antigen alone or coupled with BCR ligand (anti-IgM) for 6 h. Then, B cells were washed and incubated with a $CD4^+$ T cell hybridoma specific for MOG, and MOG antigenic presentation was evaluated by the secretion of IL-2. In UNC93B1-defective B cells, TLR signaling was abolished (Fig. 7D, left); however, significant increase in IL-2 production was detected compared to control cells even in the absence of BCR stimulation (Fig. 7D, middle). MOG peptide presentation was identical between wt and 3d cells (Fig. 7D, right). Furthermore, no difference in MHCII expression was detected between wt and

Journal of Cell Science (2020) 133, jcs236711. doi:10.1242/jcs.236711

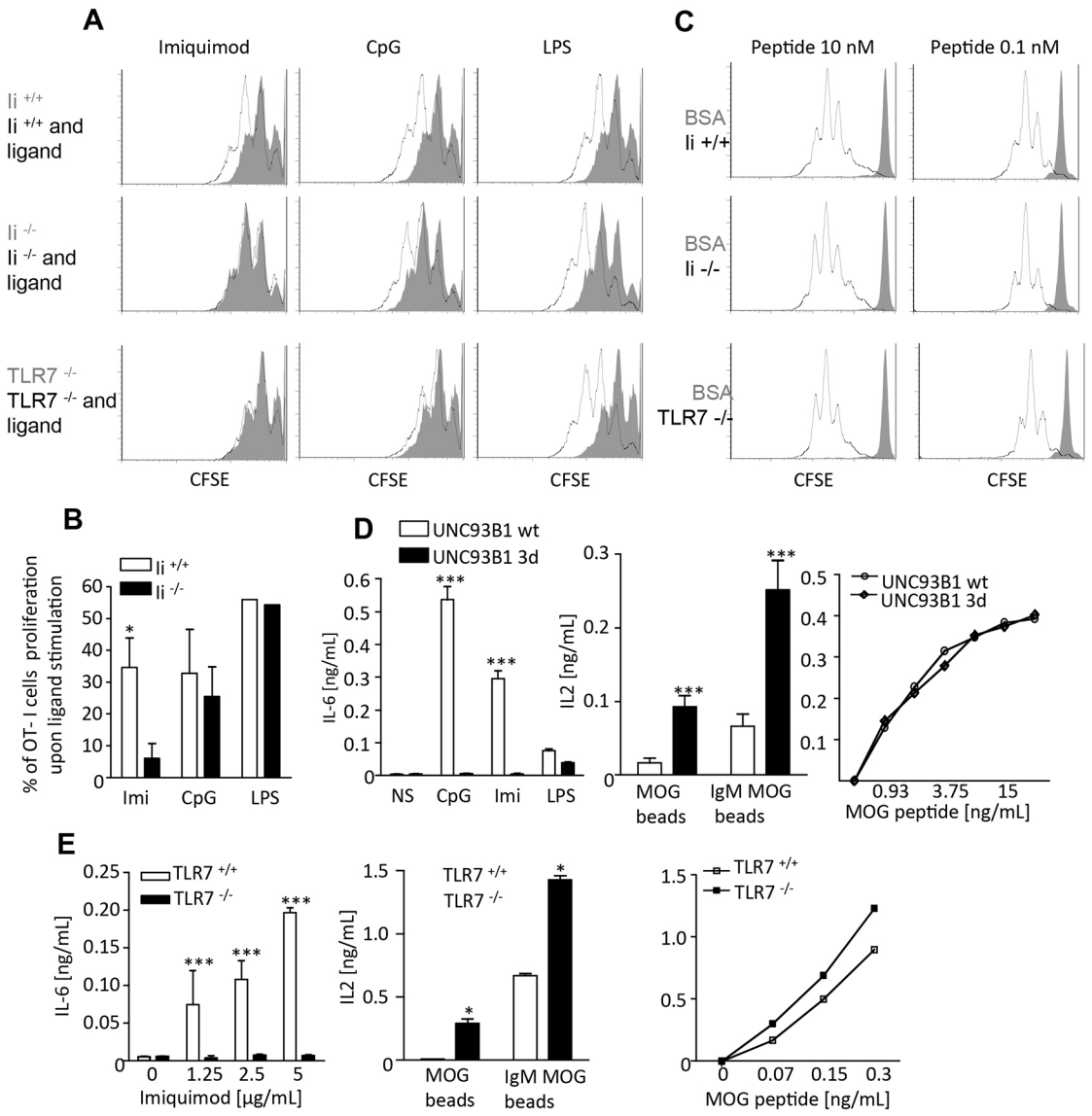

Fig. 7. Regulation of antigen presentation by Ii, UNC93B1 and TLR7. (A) Proliferation of OT-I T cells cultured with Ii$^{+/+}$, Ii$^{-/-}$ or TLR7$^{-/-}$ B cells incubated with soluble ovalbumin (gray histograms) with or without imiquimod, CpGB or LPS (dark lines). (B) Quantification of four independent experiments (mean±s.e.m., *P<0.05). (C) SIINFEKL was used as an OVA-peptide control ('Peptide') in unstimulated cells. (D) WT (white bars) and UNC93B1 mutated (black bars) B cells were stimulated with TLR ligands and IL-6 secretion was measured in the supernatants (n=3, graphs show mean±s.e.m., ***P<0.001). WT and UNC93B1 mutated (D) or TLR7$^{+/+}$ and TLR7$^{-/-}$ (E) B cells were incubated with MOG-coated beads or MOG- and IgM-coated beads for 6 h, washed and co-cultured with a CD4^{+} T cell hybridoma specific for MOG. IL-2 secretion in the supernatant was monitored by ELISA. MOG peptide was used as control (n=3, graphs show mean±s.e.m., *P<0.05, ***P<0.001). (D,E) WT or TLR7$^{+/+}$ (white bars) and UNC93B1 mutated or TLR7$^{-/-}$ (black bars) B cells were stimulated with TLR ligands and IL-6 secretion was measured in the supernatants (n=3, graphs show mean±s.e.m., ***P<0.001).

UNC93B1-defective B cells (Fig. 8A). In addition, MHCII colocalized with LAMP-1 in lysosomal compartments in wt cells, and to the same extent as in UNC93B1 mutated B cells, as shown by immunofluorescence studies (Fig. 8B). To further investigate the role of TLR7 in innate versus adaptive immunity in B cells, we stimulated TLR7-deficient B cells with TLR7 ligand and measured cytokine production and MHCII MOG antigen presentation. As expected, TLR7$^{-/-}$ B cells failed to secrete IL-6 upon imiquimod addition (Fig. 7E, left). However, MHC class II presentation was enhanced in B cells lacking TLR7 in both MOG- and MOG coupled to BCR-treated cells (Fig. 7E, middle). Again, MHCII expression and localization were similar in wt and TLR7-deficient B cells (Fig. 8C,D). However, we noticed that TLR7$^{-/-}$ B cells express slightly more Ii at the cell surface and in LAMP-1 positive lysosomes in comparison to TLR7$^{+/+}$ B cells (Fig. 8E,F). Altogether, these results show that, in B cells, TLR stimulation increases MHCI antigen cross-presentation; Ii chain promotes TLR7-dependent adaptive but not innate function; and UNC93B1 has the opposite role to Ii in favoring innate, but not adaptive, response.

DISCUSSION

The mechanisms by which intracellular TLRs are regulated remain poorly understood. Growing evidence has described the importance of a number of proteins such as the chaperone molecule UNC93B1, the MHCII complex, the clathrin adaptors (AP) and insulin responsive aminopeptidase (IRAP) in intracellular TLR trafficking, folding and signaling (Tabeta et al., 2006; Brinkmann

Journal of Cell Science (2020) 133, jcs236711. doi:10.1242/jcs.236711

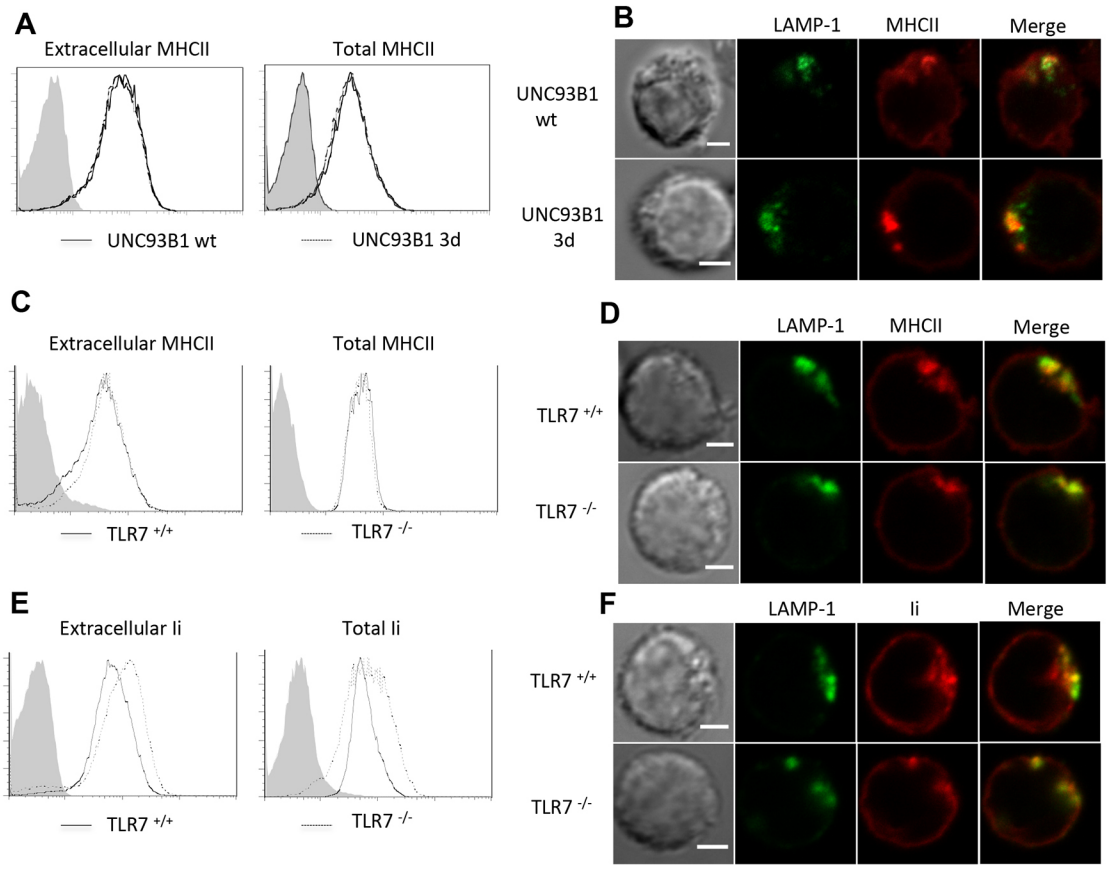

Fig. 8. MHCII and Ii chain expression and localization in TLR7- and UNC93B1-defective B cells. TLR7$^{+/+}$ (black lines), TLR7$^{-/-}$ (dashed lines) or WT (black lines), UNC93B1 mutated (dashed lines) splenic B cells were stained for MHCII (A,C) or Ii chain (E) using fluorescent antibodies. Gray histograms represent staining of B cells with the antibody isotype control. Immunofluorescence microscopy of WT, UNC93B1 mutated (B), TLR7$^{+/+}$, TLR7$^{-/-}$ (D,F) B cells immunostained for LAMP-1 (green), MHCII (red) and Ii (red). One experiment representative of three is shown. Scale bars: 5 µm.

et al., 2007; Kim et al., 2008; Sasai et al., 2010; Liu et al., 2011; Lee et al., 2011; Babdor et al., 2017).

In resting cells, TLR9 resides in the ER and, after stimulation, it is addressed to endosomal compartments (Latz et al., 2004; Leifer et al., 2004) positive for VAMP3 (Sasai et al., 2013) and IRAP (Badbor et al., 2017). There, TLR9 is cleaved and triggers the recruitment of the adaptor molecule MyD88, NF-κB activation and subsequent production of pro-inflammatory cytokines. Then, processed TLR9 is translocated to lysosomal compartments containing LAMP-1, in an AP3-dependent manner. In lysosomes, TLR9 activates IRF and the secretion of type I interferon. In UNC93B1- or AP3-deficient cells, TLR9 remains in the ER or in VAMP3-positive endosomes, whereas in DCs lacking IRAP, TLR9 is localized in LAMP-1 lysosome, leading to enhanced cytokine secretion. In addition, AP2 facilitates TLR9 transport to the cell surface and subsequent internalization in the endosomes. It has been suggested that TLR7 instead requires AP4 to travel directly from the trans-Golgi network to the endosomes, bypassing cell surface localization (Lee et al., 2013). Thus, these results indicate that identifying the specific intracellular organelles in which TLR9 resides is crucial for the outcome of the innate immune response. However, very few studies have investigated TLR7 trafficking and signaling in antigen-presenting cells, especially in B cells, probably because of the lack of antibodies specific for endogenous TLR7.

The results presented here provide evidence for a novel pathway, by which Ii chain in B cells regulates TLR7 responses by influencing the subcellular localization of TLR7. Here, we show that, in B cells, unstimulated or stimulated with TLR7 agonist, TLR7 resides in lysosomal compartments positive for MHCII, Ii chain, H-2DM and LAMP-1. In addition, the localization of TLR7 is unaltered in wt BCR cross-linked B cells. However, in Ii-deficient B cells, TLR7 relocalized partially in the ER. This suggests that expression of TLR7 in the ER might be required for the enhanced secretion of pro-inflammatory cytokines but not for the increase in MHCI antigen cross-presentation.

Two groups have recently described TLR9 trafficking and localization in B cells but nothing on TLR7 was reported. TLR7 and TLR9 trafficking require UNC93B1, a molecular chaperone, which controls their folding and transport from the ER to endolysosomes in macrophages and DCs (Kim et al., 2008; Pelka et al., 2018). Indeed, a single mutation within the UNC93B1 transmembrane domain is sufficient to abolish intracellular TLR signaling (Tabeta et al., 2006). The group of Pierce investigated endogenous TLR9 trafficking in primary B cells (Chaturvedi et al., 2008), while the group of Brinkmann generated a transgenic mouse expressing a TLR9–GFP fusion protein (Avalos et al., 2013). Pierce and colleagues reported that TLR9 resides in endosomal compartments positive for EEA1 and transferrin receptor in resting primary B cells. However, upon BCR cross-linking with labeled anti-IgM alone or together with CpG-DNA, TLR9 relocalized in LAMP-1 positive lysosomes, which contain internalized IgM (Chaturvedi et al., 2008). In contrast, the group of Brinkmann described TLR9–GFP localization in lysosomal compartments visualized by Lysotracker in resting B cells (Avalos

et al., 2013). In addition, they showed an alteration of TLR9 endosomal localization in UNC93B1-defective B cells, in which TLR9 was found in the ER and not in the lysosomes. The fact that these two groups used different tools to visualize TLR9 trafficking might account for the discrepancy observed.

Ii or CD74 is a critical chaperone for MHCII molecules (Cresswell, 1996). Ii was also shown to regulate MHCI trafficking from the ER to the endolysosomes (Basha et al., 2012). In addition, CD74 has been already characterized as an accessory signaling molecule by inducing activation of NF-κB p65/RelA homodimer and its co-activator TAF_{II} 105 and the signaling cascade involving the Syk tyrosine kinase and the PI3K/Akt pathway resulting in B-cell proliferation, survival and development (Starlets et al., 2006). Interestingly, the lack of MHCII molecules resulted in reduced TLR3, TLR4 and TLR9 signaling in macrophages and DCs (Liu et al., 2011). Following TLR3, TLR4 and TLR9 stimulation, MHCII facilitates Btk phosphorylation and interaction with CD40 in the endosomes, thus promoting pro-inflammatory cytokine production. Surprisingly, our results showed no difference in TLR4-, TLR7- and TLR9-induced pro-inflammatory cytokine secretion in both wt and MHCII-deficient B cells. However, Ii seems to selectively regulate TLR7 responses in primary B cells. In fact, we show that, in the absence of Ii, TLR7 is found in the ER together with TAP1, calreticulin and calnexin, whereas in wt cells TLR7 preferentially localizes in Ii-, H2-DM-, MHCII- and LAMP-1-positive compartments. In addition to this specific TLR7 ER localization in Ii-deficient cells, B cells lacking Ii secrete significantly more cytokines when stimulated with TLR7. In contrast, TLR9 response remains intact in Ii-deficient B cells.

Why the lack of Ii triggers significant increase in cytokine production following TLR7 stimulation is still not elucidated. Interestingly, a connection between TLR7 stimulation and the molecular chaperone calreticulin has been described by the group of Jeffries (Byrne et al., 2013). Upon TLR7 stimulation, Btk kinase is phosphorylated and associates with calreticulin. Interaction between Btk and calreticulin induces calreticulin activation and transport to the cell surface, where it colocalizes with CD91. Btk–CD91 contact will allow the cells to uptake apoptotic debris. In addition, Btk is also shown to be involved in promoting optimal TLR9-driven cytokine production in macrophages and B cells (Hasan et al., 2008; Vijayan et al., 2011). In our study, we show colocalization of TLR7 with calreticulin and calnexin in B cells lacking Ii. Thus, perhaps TLR7 stimulation in Ii-deficient B cells induces Btk phosphorylation and association with calreticulin, promoting cytokine production. In addition, Ii chain and MyD88 might compete for the binding of TLR7. Thus, in the absence of Ii chain, more MyD88 molecules might associate with TLR7, resulting in an increase in cytokine production following TLR7 stimulation. We are currently performing experiments to address this hypothesis.

By performing Duolink experiments, we show that Ii forms a complex together with MyD88, suggesting a probable role for Ii, not only in facilitating transport of TLR7 from the ER to lysosomes, but also by contributing to the signaling complex containing TLR7. In addition, Ii contains targeting motifs, two di-leucine-based signals in its cytoplasmic tail, shown to be involved in MHCII–Ii complex trafficking to early endosomes either directly or via the plasma membrane (Pond et al., 1995). Ii interacts *in vitro* with the clathrin adaptors AP1 and AP2, and these interactions are dependent on the two di-leucine-based sorting motif in its tail (Hofmann et al., 1999). Also, TLR7 transport to lysosomes might require AP4. Whether or not the same di-leucine-based motifs in Ii also interact with TLR7 with the help of AP1, AP2 or AP4 and mediate TLR7 traffic in primary B cells remains to be investigated.

Cleavage of TLR7 is critical for its activation. Previous studies have described the role of different cysteine proteases in processing TLR7 in DCs and macrophages (Ewald et al., 2011; Maschalidi et al., 2012). However, in this study, we were not able to identify the proteases cleaving TLR7 in B cells. Indeed, AEP-, cathepsin B-, cathepsin L-, cathepsin S-deficient B cells show similar cytokine production upon imiquimod stimulation (Fig. S8). Furthermore, expression of cathepsins did not differ between $Ii^{-/-}$ and $Ii^{+/+}$ B cells, indicating that TLR7 processing might not be required in B cells, or that a yet unidentified protease might be involved. Indeed, work from the group of Cerundolo describes a role for furin-like proprotein convertases in TLR7 activation in human B cells (Hipp et al., 2013). However, we did not observe any difference in cytokine production between wt B cells and B cells incubated with a specific furin inhibitor following TLR7 stimulation (data not shown).

Interestingly, Ii deficiency favors TLR7-dependent innate and not adaptive response. Indeed TLR7 does not promote MHCI antigen cross-presentation in the absence of Ii in B cells. Furthermore, in B cells lacking TLR7, Ii expression and MHCII antigen presentation are increased. Altogether, these results demonstrate a mutual regulation between TLR7 and Ii and highlight a new role for Ii in maintaining a balance between innate and adaptive responses in B cells. In addition, these results uncover a new role for Ii in modulating MHCI and MHCII, and also TLR7, transport from the ER to the lysosomes.

In conclusion, these findings suggest that targeting Ii in pathological situations in which the TLR7 pathway is dysregulated, such as diabetes and lupus, could perhaps benefit the host.

MATERIALS AND METHODS

Mice

Female or male (8- to 12-week-old) $Ii^{-/-}$, $MHCII^{-/-}$, $AEP^{-/-}$, cathepsin $B^{-/-}$, cathepsin $S^{-/-}$ and cathepsin $L^{-/-}$ mice were backcrossed ten times on the C57Bl6 background, and bred in a pathogen-free environment at Institut Necker-Enfants Malades (INEM) and Institut Curie animal facilities. All animal care and experimental procedures were performed in accordance with the guidelines and regulations of the French Veterinary Department and approved by ethical committee (A-75-2003).

Cells and stimulations

A single-cell suspension was generated by mechanical disruption of spleens from 8- to 12-week-old mice. Splenic IgM^+/IgD^+ mature B cells were isolated using a CD19-positive selection kit [Miltenyi Biotec (130-121-301), 90–95% purity as determined by fluorescence-activated cell sorting (FACS)] and immature IgM^+/IgD^- B cells were isolated and collected by flow cytometry. The mouse lymphoma cell line IIA1.6 (Lankar et al., 2002) and the MOG T-cell hybridoma (kindly provided by S. Anderton, University of Edinburgh, Edinburgh, UK) were cultured in complete RPMI medium and were authenticated and tested for contamination. BMDCs and BDDMs were generated as previously described (Sepulveda et al., 2009). Cell differentiation was controlled by FACS (anti-CD11c, HL3 and anti-CD11b, M1/70, BD Biosciences). Plated cells in 96-well plates were treated overnight with the TLR ligands (LPS from Sigma-Aldrich; imiquimod, gardiquimod and resiquimod from Invivogen; CpGB, 5′-TGACTGTGAACGTTCGAGATGA-3′, from Trilink Biotechnologies) and goat affinity purified F $(ab')_2$ anti-IgM (10 µg/ml) as a BCR ligand from MP Biomedicals. Cytokines were measured in supernatants using commercial ELISA kits (TNF-α, IL-6, eBioscience).

Preparation of antigen-coated beads

To prepare antigen-coated beads, 4×10^7 3 µm latex NH2 beads (Polyscience) were activated with 8% glutaraldehyde for 2 h at room

Journal of Cell Science (2020) 133, jcs236711. doi:10.1242/jcs.236711

temperature (RT). Beads were washed with PBS and incubated overnight (O/N) with different ligands: 100 µg/ml of F(ab′)$_2$ goat anti-mouse-IgM and 100 µg/ml of MOG or MOG protein alone.

FACS staining

Cells were permeabilized with BD Cytofix/Cytoperm and then incubated with anti-TLR7 (ab24184, Abcam, 1:100), anti-Btk (ab25971, Abcam, 1:100), anti-CD69 (552879 clone H1, 2F3, BD Biosciences, 1:100), anti-CD40 (558695, clone 3/23, BD Biosciences, 1:100), anti-MHCII (Manoury et al., 2003, Y3P antibody, 1:250) and anti-Ii (555317, clone In-1, BD Biosciences, 1:200) in PBS 1% bovine serum albumin (BSA). Cells were then analyzed by flow cytometry (FACS Calibur) using FlowJo software.

Primary B cell transfection and immunofluorescence

Splenic purified B cells were stimulated with 35 µg/ml LPS in complete RPMI medium (10% FBS, 2 mM glutamine, 50 µg/ml penicillin/streptomycin, 50 µM β-mercaptoethanol, 25 mM HEPES, 1× non-essential amino acids, 1 mM sodium pyruvate) overnight at a concentration of 2×10^6 cells/ml. Then, 5×10^6 B cells were transfected with 2.5 µg cDNA coding for mouse full-length TLR7-HA tagged or for mouse full-length TLR9–GFP using a mouse B cell Amaxa kit (Lonza, Germany). Twenty-four hours later, cells were harvested and stimulated with TLR7, TLR9 ligands and/or BCR ligand for different times. For immunofluorescence studies, transfected B cells were grown on IBIDI channels (Biovalley) for 2 h, then stimulated and fixed with 4% paraformaldehyde for 10 min at RT and quenched in 100 mM glycine for 5 min. Fixed cells were permeabilized for 20 min and incubated at RT with anti-HA (3F10 clone, Sigma-Aldrich, 1:100), anti-GFP (1814460, Roche, 1:100), anti-H2DM (gift from D. lankar, Institut Curie, Paris, France), anti-calreticulin (ab2907, Abcam, 1:200), anti-ERGIC-53 (ab129179, Abcam, 1:100), anti-Ii (555317, clone In-1, BD Biosciences, 1:100), anti-UNC93B1 (sc-135545, Santa Cruz Biotechnology, 1:100), anti-TAP1 (sc-11465, Santa Cruz Biotechnology, 1:100), anti-MHCII (Manoury et al., 2003, Y3P clone, 1:200), anti-VAMP3 (104203, Synaptic Systems, 1:100) and anti-CD107α LAMP1 (553792, clone 1D4B, BD Biosciences, 1:200) antibodies in PBS, 0.2% BSA, 0.05% saponin for 1 h. Secondary antibodies (anti-mouse, anti-rat and anti-rabbit; 1:250) are from Jackson ImmunoResearch. Immunofluorescence images were acquired on a Zeiss confocal microscope (laser scanning confocal microscope LSM700; 63×/1.4 NA oil DicM27 plan apochromat objective) with the acquisition software Zen 2009, and were analysed and quantified with ImageJ software.

Lysotracker staining

Splenic B cells (2×10^5) were grown on IBIDI channels (Biovalley) for 2 h in complete RPMI medium and were incubated with 75 nM Lysotracker Red (Molecular Probes, Invitrogen) for 30 min at 37°C. Time-lapse images were obtained every 10 min for 2 h with a Zeiss LSM confocal microscope.

In situ proximity ligation assay (PLA)

A Duolink *in situ* PLA kit was used according to the manufacturer's instructions (Olink, Biosciences) for *in situ* PLAs. Briefly, B cells were grown on coverslips and then fixed in 4% paraformaldehyde for 10 min before permeabilization in PBS, 0.05% saponin-0.2% BSA for 10 min. Cells were then blocked in 3% BSA/PBS and incubated with primary antibodies (anti-MyD88, D80F5, Cell Signaling Technology; anti-NF-κB, sc-372, Santa Cruz Biotechnology; anti-HA, CF29F4, Sigma-Aldrich; anti-Ii, 555317, clone In-1, BD Biosciences, and anti-GFP, ab290, Abcam; all at 1:100 dilution). After washing the cells, PLA probes were added, followed by hybridization, ligation and amplification for 90 min at 37°C. TLR7–Ii, MyD88–Ii, TLR9–Ii, Myd88–NF-κB and MHCII–Ii interactions (red) were visualized after incubation with the detection solution. Slides were analyzed by confocal microscopy. Quantification of mean fluorescence was performed using ImageJ software.

Real-time polymerase chain reaction

Total RNA was extracted from 5×10^6 splenic mature B cells using an RNeasy Mini Kit according to manufacturer's instructions (Qiagen). Corresponding cDNA was synthesized using a reverse transcriptase kit from Promega. Real-time polymerase chain reaction (RT-PCR) was then performed using an ABI 7900 RT-PCR detection system (Applied Biosystems, Foster City, CA) in 10 µl reactions containing 1 µl of diluted cDNA, 300 nM of forward and reverse primers and SYBR Green PCR Master Mix (Thermo Fisher Scientific). Each sample was run in duplicate for *Tlr7* gene and the relative quantity (RQ) of mRNA was calculated based on the housekeeping gene *Hprt*. The sequences of the primers used are the following: Fw: 5′-CAGGCCAGATTTGTTGGAT-3′; Rv: 5′-TTGCGCTCATCTTAGGCTTT-3′ for mouse *Hprt* and Fw: 5′-CCACAGGCTCACCCATACTTC-3′; Rv: 5′-GGGATGTCCTAGGTGGTGACA-3′ for murine *Tlr7*.

Antigen presentation assays

In vitro cross-presentation assays were performed as previously described (Maschalidi et al., 2017). Briefly, Ii$^{+/+}$, Ii$^{-/-}$ and TLR7$^{-/-}$ splenic B cells were incubated with 10 mg of soluble OVA or BSA and stimulated or not with 10 µg/ml imiquimod, 10 µg/ml CpGB or 1 µg/ml LPS. Then, CFSE-labeled OT-I T cells were added to the culture and the proliferation of T cells was monitored 3 days later. MOG antigen was coupled to glutaraldehyde-activated NH2 beads together with or without F(ab′)$_2$ anti-mouse-IgM in equal concentrations. Spleen mature B (2×10^5 cells/well) cells from wt, UNC93B1 mutated and TLR7$^{-/-}$ mice were incubated with MOG-coated beads in the presence or absence of F(ab′)$_2$ anti-mouse-IgM or with MOG peptide for 6 h at 37°C in 96-well plates. B cells were then washed and incubated with 10^5 MOG T-cell hybridoma for 24 h. IL-2 was measured in the supernatants using an ELISA kit from BD Biosciences.

Lentivirus infection

For shRNA experiments, purified pLKO.1 lentiviral plasmids carrying shRNA sequences for Ii (NM_010545, Sigma-Aldrich) or control shRNA (SHC002, Sigma-Aldrich) were used to generate lentiviral particles. Briefly, HEK 293T packaging cells were co-transfected with the transfer (pLKO/shRNA), packaging (pPAX2) and envelope (pMD2G) plasmids, using GeneJuice Transfection Reagent (Novagen) as recommended by the manufacturer. Virus supernatant was titered and added to the cell culture containing the IIA1.6 B cell line at day 2 and at a multiplicity of 0.03 pg p24/cell. The medium was changed at day 3 and infected cells were selected with 4.5 µg/ml of puromycin added in the medium from day 4 to day 6. Several washes were done during the selection process to eliminate dead cells. Infected B cells were used for Duolink experiments and western blot analysis.

Constructs

Murine *Tlr7* and *Tlr9* constructs were generated as previously described (Sepulveda et al., 2009; Maschalidi et al., 2012). Briefly, *Tlr7* and *Tlr9* cDNAs containing the FL sequence followed by a HA tag or GFP tag were cloned into pcDNA3.1 by PCR of the pUNO mTLR7-HA or pUNO mTLR9-HA plasmid (Invivogen).

Imaging flow cytometry analysis (Imagestream)

Purified spleen B cells (3×10^6) were first incubated in complete medium for 30 min at 37°C with or without TLR7 ligand (guardiquimod 1 µg/ml). Cells were then placed on ice and washed with FACS buffer (PBS, 5 mM EDTA, 3% fetal calf serum) before fixation and permeabilization using a BD Cytofix/Cytoperm kit (BD Biosciences) for 2 h. Fixed and permeabilized cells were incubated at room temperature for 30 min with anti-LAMP-1 (553792, clone 1D4B, Pharmingen, 1:200), anti-calnexin (kindly provided by E. Chevet, University of Rennes, Rennes, France, 1:200), anti-UNC93B1 and anti-TLR7 PE (565557, clone A94B10, BD Biosciences, 1:100). Secondary antibodies anti-rat Alexa Fluor 488 (712-605-143, Jackson ImmunoResearch, 1:200) and anti-rabbit Alexa Fluor 647 (711-545-152, Jackson ImmunoResearch, 1:100) antibodies were then added for 30 min at 4°C in the dark. After washing, cells were stained with 4′,6-diamidino-2-phenylindole (DAPI) and image acquisition was performed. Samples were run on an Imagestream ISX mkII (Amnis Corp, Luminex, Seattle, WA) and 60× magnification was used for all acquisitions. Data were acquired using the INSPIRE software (Amnis Corp) and analyzed using IDEAS™ software (version 6.2 Amnis Corp). On average, 30,000–50,000 events were

collected in all experiments. Single-stain controls were run for each fluorochrome used and spectral compensation was performed. Cells were gated for single cells using the area and aspect ratio of the brightfield image, gated for focused cells using the gradient RMS feature, and viable cells were selected on the basis of positive expression of DAPI. LAMP-1, CNX and UNC93B1 masks were created to study the localization and expression of TLR7. TLR7 quantification was expressed as mean pixel intensity value, which is the intensity normalized to the surface area of the mask for each compartment. Normalization between $Ii^{+/+}$, $Ii^{-/-}$ was done by dividing this value by the mean pixel intensity of TLR7 of the mask of the whole cell.

Statistics

Statistical significance was determined by unpaired Student's *t*-test or two-way ANOVA. $*P<0.05$, $**P<0.01$ and $***P<0.001$.

Acknowledgements

We are grateful to S. Akira (Osaka, Japan) and N. Doyen (Institut Pasteur, France) for providing the $TLR7^{-/-}$ mice, and to the animal facility of the Institut Curie for hosting $Ii^{-/-}$ mice. The UNC93B1 mutated mice (3d) were kindly provided by Dr B. Ryffel (CDTA, Orléans). We also thank N. Goudin, R. Desvaux and M. Garfa-Traore (Plateforme d'Imagerie Dynamique, Institut Necker, France) for their help with the confocal microscope and F. X. Mauvais (INEM, France) for advice on imaging flow cytometry. Cell sorting of immature B cells was performed with the help of S. Korniotis (UMR 8147, France).

Competing interests

The authors declare no competing or financial interests.

Author contributions

Conceptualization: M.T., M.D., S.M., B.M.; Methodology: M.T., L.M., K.A., M.D., S.M., B.M.; Validation: M.T., B.M.; Investigation: M.T.; Resources: B.M.; Writing - original draft: B.M.; Supervision: B.M.; Funding acquisition: B.M.

Funding

This study was supported by a grant from Agence Nationale de la Recherche [MIDI 008 01 to B.M.] and PhD fellowships from Association de Recherche contre le Cancer, Institut Curie and Ministére de la Recherche et de la Technologie to S.M., M.T. and L.M., respectively.

Supplementary information

Supplementary information available online at
http://jcs.biologists.org/lookup/doi/10.1242/jcs.236711.supplemental

References

Avalos, A. M., Kirak, O., Oelkers, J. M., Pils, M. C., Kim, Y.-M., Ottinger, M., Jaenisch, R., Ploegh, H. L. and Brinkmann, M. M. (2013). Cell-specific TLR9 trafficking in primary APCs of transgenic TLR9-GFP mice. *J. Immunol.* **190**, 695-702. doi:10.4049/jimmunol.1202342

Babdor, J., Descamps, D., Adiko, A. C., Tohmé, M., Maschalidi, S., Evnouchidou, I., Vasconcellos, L. R., De Luca, M., Mauvais, F.-X., Garfa-Traore, M. et al. (2017). $IRAP^+$ endosomes restrict TLR9 activation and signaling. *Nat. Immunol.* **18**, 509-518. doi:10.1038/ni.3711

Basha, G., Omilusik, K., Chavez-Steenbock, A., Reinicke, A. T., Lack, N., Choi, K. B. and Jefferies, W. A. (2012). A CD74-dependent MHC class I endolysosomal cross-presentation pathway. *Nat. Immunol.* **13**, 237-245. doi:10.1038/ni.2225

Brinkmann, M. M., Spooner, E., Hoebe, K., Beutler, B., Ploegh, H. L. and Kim, Y.-M. (2007). The interaction between the ER membrane protein UNC93B and TLR3, 7, and 9 is crucial for TLR signaling. *J. Cell. Biol.* **177**, 265-275. doi:10.1083/jcb.200612056

Byrne, J. C., Ní Gabhann, J., Stacey, K. B., Coffey, B. M., McCarthy, E., Thomas, W. and Jefferies, C. A. (2013). Bruton's tyrosine kinase is required for apoptotic cell uptake via regulating the phosphorylation and localization of calreticulin. *J. Immunol.* **190**, 5207-5215. doi:10.4049/jimmunol.1300057

Caetano, B. C., Carmo, B. B., Melo, M. B., Cerny, A., Dos Santos, S. L., Bartholomeu, D. C., Golenbock, D. T. and Gazzinelli, R. T. (2011). Requirement of UNC93B1 reveals a critical role for TLR7 in host resistance to primary infection with Trypanosoma cruzi. *J. Immunol.* **187**, 1903-1911. doi:10.4049/jimmunol.1003911

Casrouge, A., Zhang, S.-Y., Eidenschenk, C., Jouanguy, E., Puel, A., Yang, K., Alcais, A., Picard, C., Mahfoufi, N., Nicolas, N. et al. (2006). Herpes simplex virus encephalitis in human UNC-93B deficiency. *Science* **314**, 308-312. doi:10.1126/science.1128346

Chaturvedi, A., Dorward, D. and Pierce, S. K. (2008). The B cell receptor governs the subcellular location of Toll-like receptor 9 leading to hyperresponses to DNA-containing antigens. *Immunity* **28**, 799-809. doi:10.1016/j.immuni.2008.03.019

Cresswell, P. (1996). Invariant chain structure and MHCII function. *Cell* **4**, 505-507. doi:10.1016/s0092-8674(00)81025-9

Denzin, L. K. and Cresswell, P. (1995). HLA-DM induces CLIP dissociation from MHC class II αβ dimers and facilitates peptide loading. *Cell* **82**, 155-165. doi:10.1016/0092-8674(95)90061-6

Ewald, S. E., Engel, A., Lee, J., Wang, M., Bogyo, M. and Barton, G. M. (2011). Nucleic acid recognition by Toll-like receptors is coupled to stepwise processing by cathepsins and asparagine endopeptidase. *J. Exp. Med.* **4**, 643-651. doi:10.1084/jem.20100682

Ewald, S. E., Lee, B. L., Lau, L., Wickliffe, K. E., Shi, G.-P., Chapman, H. A. and Barton, G. M. (2008). The ectodomain of Toll-like receptor 9 is cleaved to generate a functional receptor. *Nature* **456**, 658-662. doi:10.1038/nature07405

Hasan, M., Lopez-Herrera, G., Blomberg, K. E. M., Lindvall, J. M., Berglöf, A., Smith, C. I. E. and Vargas, L. (2008). Defective Toll-like receptor 9-mediated cytokine production in B cells from Bruton's tyrosine kinase-deficient mice. *Immunology* **123**, 239-249. doi: 10.1111/j.1365-2567.2007.02693.x

Heit, A., Huster, K. M., Schmitz, F., Schiemann, M., Busch, D. H. and Wagner, H. (2004). CpG-DNA aided cross-priming by cross-presenting B cells. *J. Immunol.* **172**, 1501-1507. doi:10.4049/jimmunol.172.3.1501

Hemmi, H., Kaisho, T., Takeuchi, O., Sato, S., Sanjo, H., Hoshino, K., Horiuchi, T., Tomizawa, H., Takeda, K. and Akira, S. (2002). Small anti-viral compounds activate immune cells via the TLR7 MyD88-dependent signaling pathway. *Nat. Immunol.* **3**, 196-200. doi:10.1038/ni758

Hipp, M. M., Shepherd, D., Gileadi, U., Aichinger, M. C., Kessler, B. M., Edelmann, M. J., Essalmani, R., Seidah, N. G., Reis e Sousa, C. and Cerundolo, V. (2013). Processing of human toll-like receptor 7 by Furin-like proprotein convertases is required for its accumulation and activity in endosomes. *Immunity* **39**, 711-721. doi:10.1016/j.immuni.2013.09.004

Hofmann, M. W., Höning, S., Rodionov, D., Dobberstein, B., von Figura, K. and Bakke, O. (1999). The leucine-based sorting motifs in the cytoplasmic domain of the invariant chain are recognized by the clathrin adaptors AP1 and AP2 and their medium chains. *J. Biol. Chem.* **274**, 36153-36158. doi:10.1074/jbc.274.51.36153

Jiang, W., Lederman, M. M., Harding, C. V. and Sieg, S. F. (2011). Presentation of soluble antigens to $CD8^+$ T cells by CpG oligodeoxynucleotide-primed human naive B cells. *J. Immunol.* **186**, 2080-2086. doi:10.4049/jimmunol.1001869

Ke, Y. and Kapp, J. A. (1996). Exogenous antigens gain access to the major histocompatibility complex class I processing pathway in B cells by receptor-mediated uptake. *J. Exp. Med.* **184**, 1179-1184. doi:10.1084/jem.184.3.1179

Kim, Y.-M., Brinkmann, M. M., Paquet, M.-E. and Ploegh, H. L. (2008). UNC93B1 delivers nucleotide-sensing toll-like receptors to endolysosomes. *Nature* **452**, 234-238. doi:10.1038/nature06726

Lankar, D., Vincent-Schneider, H., Briken, V., Yokozeki, T., Raposo, G. and Bonnerot, C. (2002). Dynamics of major histocompatibility complex class II compartments during B cell receptor-mediated cell activation. *J. Exp. Med.* **195**, 461-472. doi:10.1084/jem.20011543

Latz, E., Schoenemeyer, A., Visintin, A., Fitzgerald, K. A., Monks, B. G., Knetter, C. F., Lien, E., Nilsen, N. J., Espevik, T. and Golenbock, D. T. (2004). TLR9 signals after translocating from the ER to CpG DNA in the lysosome. *Nat. Immunol.* **5**, 190-198. doi:10.1038/ni1028

Lee, B. L., Moon, J. E., Shu, J. H., Yuan, L., Newman, Z. R., Schekman, R. and Barton, G. M. (2013). UNC93B1 mediates differential trafficking of endosomal TLRs. *eLife* **2**, e00291. doi:10.7554/eLife.00291

Leifer, C. A., Kennedy, M. N., Mazzoni, A., Lee, C. W., Kruhlak, M. J. and Segal, D. M. (2004). TLR9 is localized in the endoplasmic reticulum prior to stimulation. *J. Immunol.* **173**, 1179-1183. doi:10.4049/jimmunol.173.2.1179

Leuchowius, K.-J., Weibrecht, I. and Söderberg, O. (2011). In situ proximity ligation assay for microscopy and flow cytometry. *Curr. Protoc. Cytom.* **56**, 9.36.1-9.36.15. doi:10.1002/0471142956.cy0936s56

Liu, X., Zhan, Z., Li, D., Xu, L., Ma, F., Zhang, P., Yao, H. and Cao, X. (2011). Intracellular MHC class II molecules promote TLR-triggered innate immune responses by maintaining activation of the kinase Btk. *Nat. Immunol.* **12**, 416-424. doi:10.1038/ni.2015

Lund, J. M., Alexopoulou, L., Sato, A., Karow, M., Adams, N. C., Gale, N. W., Iwasaki, A. and Flavell, R. A. (2004). Recognition of single-stranded RNA viruses by Toll-like receptor 7. *Proc. Natl. Acad. Sci. USA* **101**, 5598-5603. doi:10.1073/pnas.0400937101

Majer, O., Liu, B., Woo, B. J., Kreuk, L. S. M., Van Dis, E. and Barton, G. M. (2019). Release from UNC93B1 reinforces the compartmentalized activation of select TLRs. *Nature* **575**, 371-374. doi:10.1038/s41586-019-1611-7

Manoury, B., Mazzeo, D., Li, D. N., Billson, J., Loak, K., Benaroch, P. and Watts, C. (2003). Asparagine endopeptidase can initiate the removal of the MHC class II invariant chain chaperone. *Immunity* **4**, 489-498. doi:10.1016/S1074-7613(03)00085-2

Maschalidi, S., Hässler, S., Blanc, F., Sepulveda, F. E., Tohme, M., Chignard, M., van Endert, P., Si-Tahar, M., Descamps, D. and Manoury, B. (2012). Asparagine endopeptidase controls anti-influenza virus immune responses

through TLR7 activation. *PLoS. Pathog.* **8**, e1002841. doi:10.1371/journal.ppat.1002841

Maschalidi, S., Nunes-Hasler, P., Nascimento, C. R., Sallent, I., Lannoy, V., Garfa-Traore, M., Cagnard, N., Sepulveda, F. E., Vargas, P., Lennon-Duménil, A.-M. et al. (2017). UNC93B1 interacts with the calcium sensor STIM1 for efficient antigen cross-presentation in dendritic cells. *Nat. Commun.* **8**, 1640. doi:10.1038/s41467-017-01601-5

Matsumoto, F., Saitoh, S.-I., Fukui, R., Kobayashi, T., Tanimura, N., Konno, K., Kusumoto, Y., Akashi-Takamura, S. and Miyake, K. (2008). Cathepsins are required for Toll-like receptor 9 responses. *Biochem. Biophys. Res. Commun.* **367**, 693-699. doi:10.1016/j.bbrc.2007.12.130

Melo, M. B., Kasperkovitz, P., Cerny, A., Könen-Waisman, S., Kurt-Jones, E. A., Lien, E., Beutler, B., Howard, J. C., Golenbock, D. T. and Gazzinelli, R. T. (2010). UNC93B1 mediates host resistance to infection with Toxoplasma gondii. *PLoS. Pathog.* **6**, e1001071. doi:10.1371/journal.ppat.1001071

Misawa, T., Takahama, M., Kozaki, T., Lee, H., Zou, J., Saitoh, T. and Akira, S. (2013). Microtubule-driven spatial arrangement of mitochondria promotes activation of the NLRP3 inflammasome. *Nat. Immunol.* **14**, 454-460. doi:10.1038/ni.2550

Park, B., Brinkmann, M. M., Spooner, E., Lee, C. C., Kim, Y.-M. and Ploegh, H. L. (2008). Proteolytic cleavage in an endolysosomal compartment is required for activation of Toll-like receptor 9. *Nat. Immunol.* **9**, 1407-1414. doi:10.1038/ni.1669

Pelka, K., Bertheloot, D., Reimer, E., Phulphagar, K., Schmidt, S. V., Christ, A., Stahl, R., Watson, N., Miyake, K., Hacohen, N. et al. (2018). The chaperone UNC93B1 regulates toll-like receptor stability independently of endosomal TLR transport. *Immunity* **48**, 911-922.e7. doi:10.1016/j.immuni.2018.04.011

Pond, L., Kuhn, L. A., Teyton, L., Schutze, M.-P., Tainer, J. A., Jackson, M. R. and Peterson, P. A. (1995). A role for acidic residues in di-leucine motif-based targeting to the endocytic pathway. *J. Biol. Chem.* **270**, 19989-19997. doi:10.1074/jbc.270.34.19989

Roche, P. A., Marks, M. S. and Cresswell, P. J. (1991). Formation of a nine-subunit complex by HLA class II glycoproteins and the invariant chain. *Nature* **354**, 392-394. doi:10.1038/354392a0

Sasai, M., Linehan, M. M. and Iwasaki, A. (2010). Bifurcation of Toll-like receptor 9 signaling by adaptor protein 3. *Science* **329**, 1530-1534. doi:10.1126/science.1187029

Sepulveda, F. E., Maschalidi, S., Colisson, R., Heslop, L., Ghirelli, C., Sakka, E., Lennon-Duménil, A.-M., Amigorena, S., Cabanie, L. and Manoury, B. (2009). Critical role for asparagine endopeptidase in endocytic Toll-like receptor signaling in dendritic cells. *Immunity* **31**, 737-748. doi:10.1016/j.immuni.2009.09.013

Starlets, D., Gore, Y., Binsky, I., Haran, M., Harpaz, N., Shvidel, L., Becker-Herman, S., Berrebi, A. and Shachar, I. (2006). Cell-surface CD74 initiates a signaling cascade leading to cell proliferation and survival. *Blood* **107**, 4807-4816. doi:10.1182/blood-2005-11-4334

Tabeta, K., Hoebe, K., Janssen, E. M., Du, X., Georgel, P., Crozat, K., Mudd, S., Mann, N., Sovath, S., Goode, J. et al. (2006). The Unc93b1 mutation 3d disrupts exogenous antigen presentation and signaling via Toll-like receptors 3, 7 and 9. *Nat. Immunol.* **7**, 156-164. doi:10.1038/ni1297

Teyton, L. and Peterson, P. A. (1992). Invariant chain–a regulator of antigen presentation. *Trends Cell. Biol.* **2**, 52-56. doi:10.1016/0962-8924(92)90163-H

Vijayan, V., Baumgart-Vogt, E., Naidu, S., Qian, G. and Immenschuh, S. (2011). Bruton's tyrosine kinase is required for TLR-dependent heme oxygenase-1 gene activation via Nrf2 in macrophages. *J. Immunol.* **187**, 817-827. doi:10.4049/jimmunol.1003631

Viville, S., Neefjes, J., Lotteau, V., Dierich, A., Lemeur, M., Ploegh, H., Benoist, C. and Mathis, D. (1993). Mice lacking the MHC class II-associated invariant chain. *Cell* **72**, 635-648. doi:10.1016/0092-8674(93)90081-Z

Yamazaki, T., Yoshimatsu, Y., Morishita, Y., Miyazono, K. and Watabe, T. (2009). COUP-TFII regulates the functions of Prox1 in lymphatic endothelial cells through direct interaction. *Genes Cells* **14**, 425-434. doi:10.1111/j.1365-2443.2008.01279.x

Zhong, G., Romagnoli, P. and Germain, R. N. (1997). Related leucine-based cytoplasmic targeting signals in invariant chain and major histocompatibility complex class II molecules control endocytic presentation of distinct determinants in a single protein. *J. Exp. Med.* **185**, 429-438. doi:10.1084/jem.185.3.429

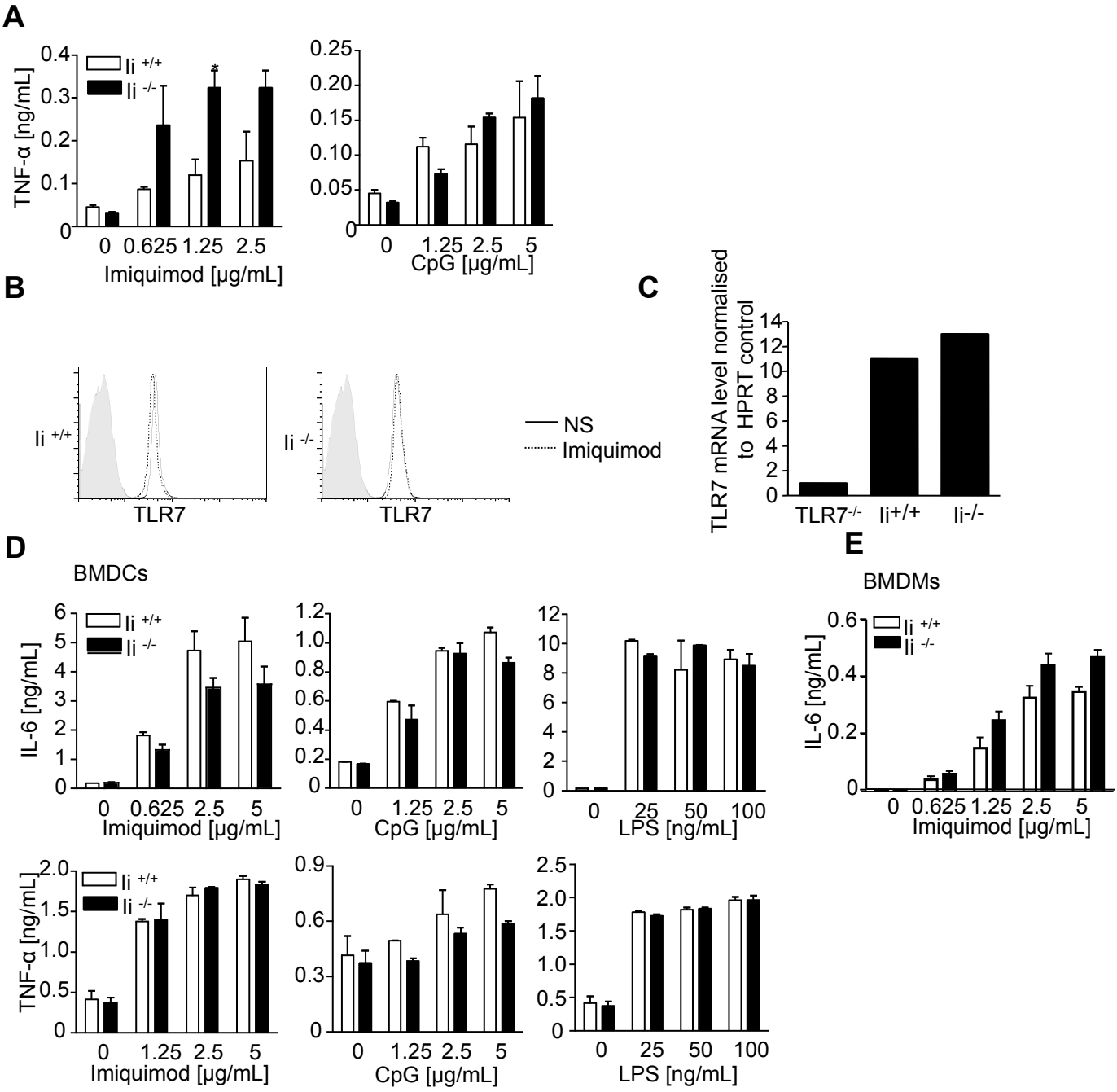

Fig S1. TLR7 stimulation increases TNFα production specifically in Ii chain deficient B cells. (A) $Ii^{+/+}$ or $Ii^{-/-}$ mature splenic B cells were stimulated with different TLRs ligands for 12h and secretion of TNF-α was measured by ELISA. (n=8, graphs show mean ± SEM, *p <0.05). (**B**) $Ii^{+/+}$ or $Ii^{-/-}$ mouse splenic B cells were treated without (black lines) or with (dashed lines) 5 μg/ml of imiquimod for 16h and stained for TLR7 expression using fluorescent antibody. Grey histograms represent staining of B cells with the antibody isotype control. One experiment representative out of two is shown (**C**) TLR7 mRNA level was monitored by quantitative real-time PCR from total RNA extracted from $Ii^{+/+}$, $Ii^{-/-}$ and $TLR7^{-/-}$ resting mature splenic B cells. One experiment representative out of two is shown. IL-6 and TNF-α production from Ii wt or Ii-deficient BMDCs (**D**) and IL-6 production from Ii wt or Ii-deficient BMDMs (**E**) incubated with different TLRs ligands. Cytokine production was measured by ELISA. (n=3, graphs show mean ± SEM).

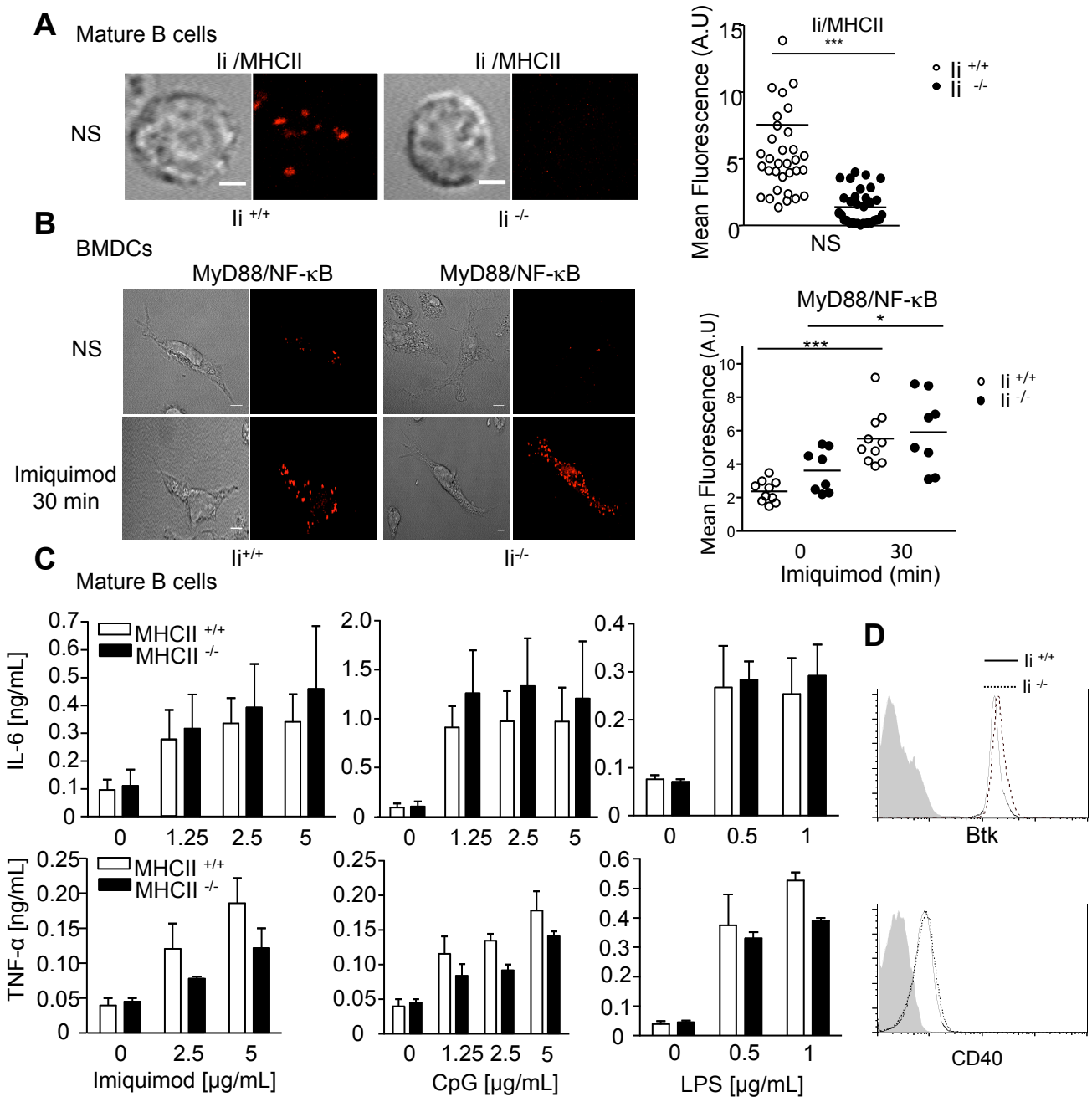

Fig S2. TLR7 stimulation leads to similar cytokine production in MHCII wt and deficient B cells. (**A**) Detection of Ii and MHCII interaction using PLA *in situ* with anti MHCII and anti Ii specific mAbs in resting splenic mature B cells. PLA signals are shown in red. One representative experiment out of three is shown. Quantification of mean fluorescence using Image J software (n=30-35 cells, ***p< 0.001). (**B**) Detection of Myd88 and NF-κB interaction using PLA *in situ* with specific mAbs in wt- and Ii- deficient BMDCs stimulated or not with imiquimod for 30 minutes. PLA signals are shown in red. One representative experiment out of three is shown. Quantification of mean fluorescence using Image J software (n=10 cells, *p< 0.05, ***p< 0.001). (**C**) IL-6 and TNF-α production by $MHCII^{+/+}$ or $MHCII^{-/-}$ mature splenic B cells incubated with different TLRs ligands. Cytokine production was measured by ELISA (n=3, graphs show mean ± SEM). (**D**) $Ii^{+/+}$ (black lines) or $Ii^{-/-}$ (dashed lines) mouse splenic B cells were stained for Btk or CD40 expression using fluorescent antibodies. Grey histograms represent staining of B cells with the antibody isotype control. NS: not stimulated.

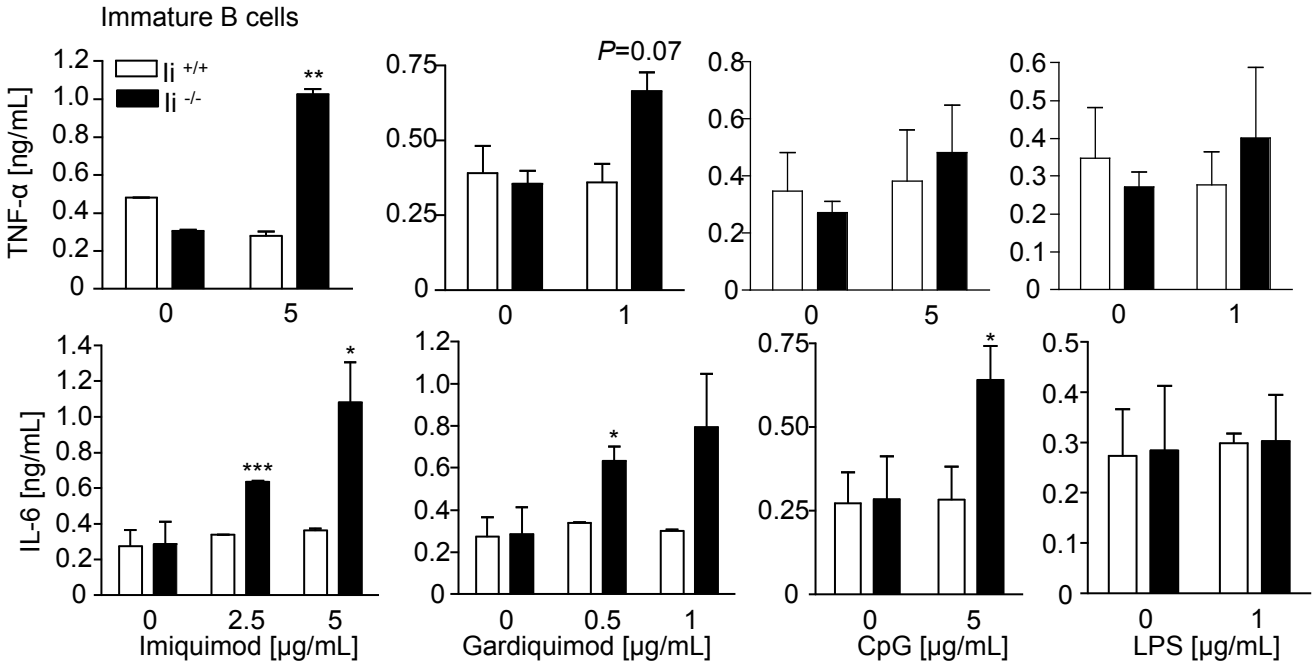

Fig S3. TLR7 signaling is increased in Ii chain deficient immature bone marrow B cells. Immature bone marrow B cells from $Ii^{-/-}$ or $Ii^{+/+}$ were activated with different TLRs ligands and cytokine secretion was measured by ELISA. (n=3, graphs show mean ± SEM, *p< 0.05,** p< 0.01).

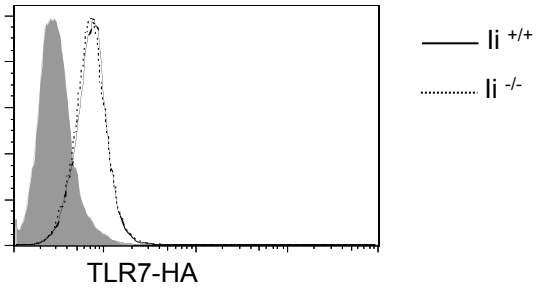

Fig S4. $Ii^{+/+}$ and $Ii^{-/-}$ B cells display similar transfected TLR7-HA expression. $Ii^{+/+}$ or $Ii^{-/-}$ mature splenic B cells were transfected with a cDNA coding for FL TLR7 tagged HA. TLR7 expression was assessed 48h after transfection by flow cytometry with an anti-HA specific antibody (black or dotted lines) or with the antibody isotype control (grey histograms). One experiment out of three is shown (mean of three experiments, expression of TLR7 in $Ii^{+/+}$: 27% and in $Ii^{-/-}$: 32%).

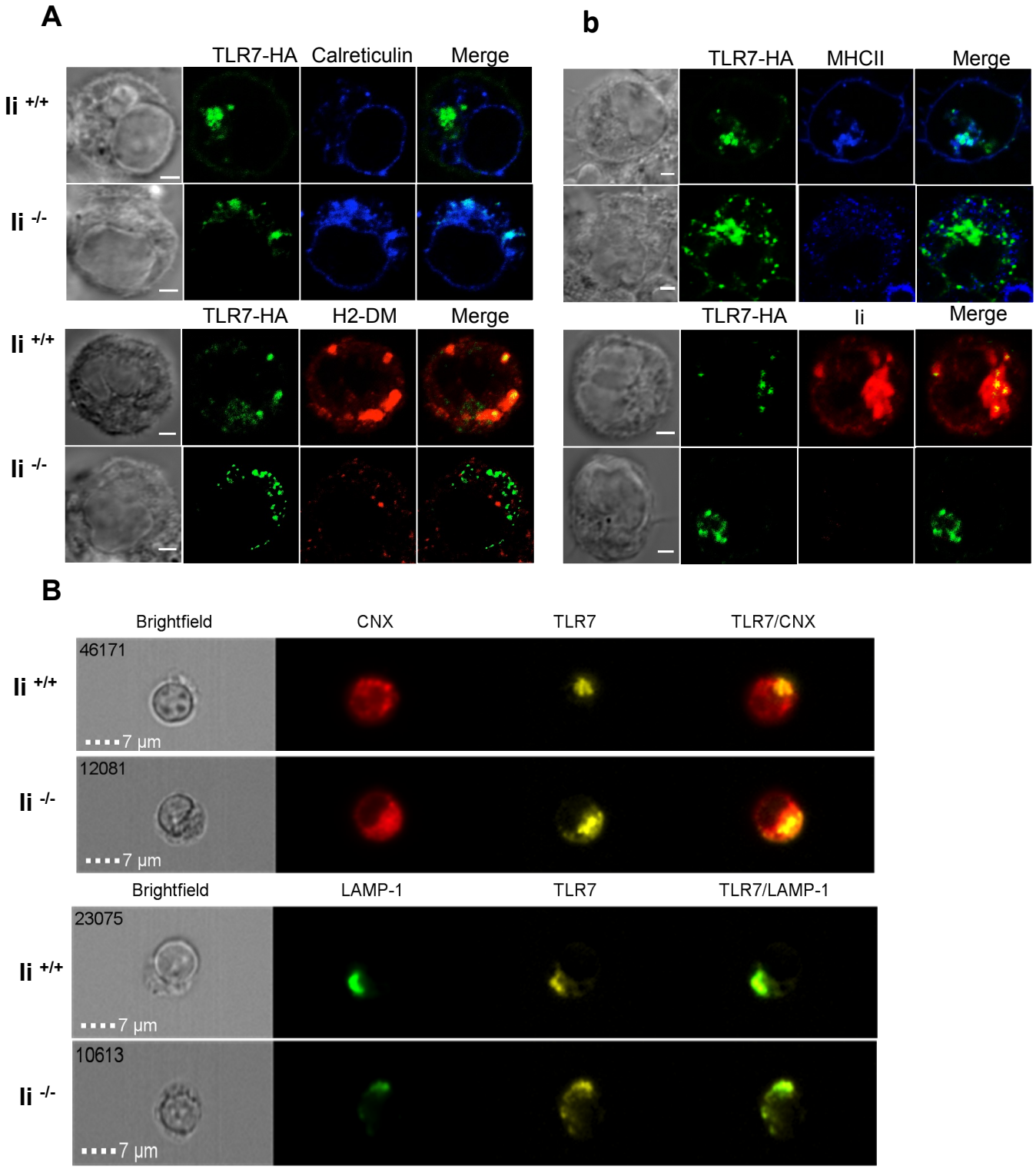

Fig S5. Ii regulates TLR7 trafficking in B cells. (**A**) Immunofluorescence microscopy of TLR7-stimulated $Ii^{+/+}$ or $Ii^{-/-}$ splenic B cells transfected with FL TLR7 tagged HA and stained for TLR7 (green), calreticulin (blue), H2-DM (red), MHCII (blue) and Ii (red). One experiment representative out of three is shown. (**B**) Representative images of calnexin (CNX), LAMP-1, and TLR7 intracellular staining in TLR7-stimulated B cells from Ii+/+ or $Ii^{-/-}$ acquired by imaging flow cytometry.One experiment representative out of three is shown.

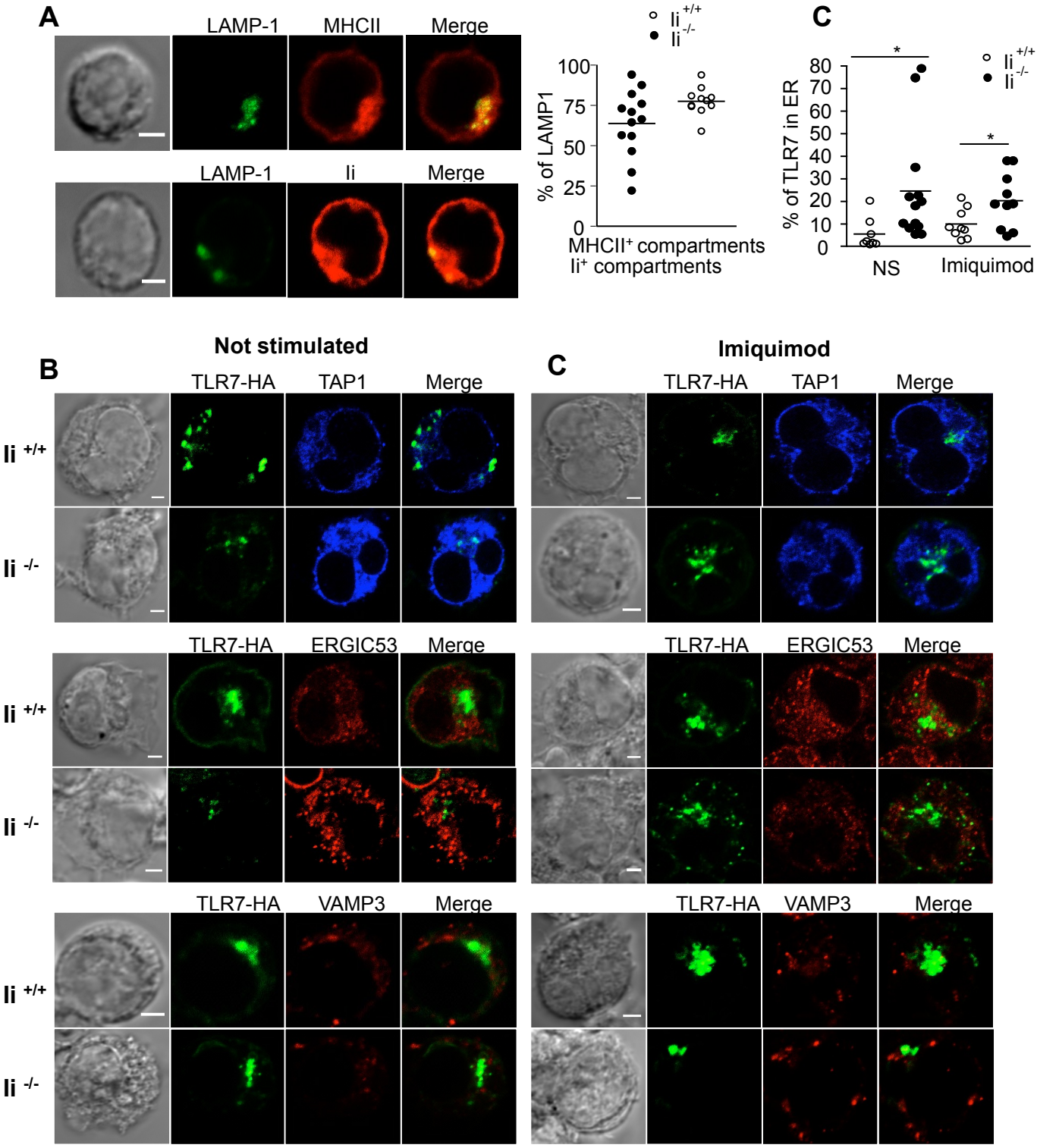

Fig S6. TLR7 is expressed in ER in Ii deficient B cells. (**A**) Immunofluorescence microscopy of resting $Ii^{+/+}$ splenic B cells stained for LAMP1 (green), MHCII (red) and Ii (red), left panel. One experiment representative out of three is shown (left panel). (**B**) Immunofluorescence microscopy of resting or TLR7-stimulated $Ii^{+/+}$ or $Ii^{-/-}$ splenic B cells transfected with FL TLR7 tagged HA and stained for TLR7 (green), TAP1 (blue), ERGIC 53 (red) and VAMP3 (red). One experiment representative out of three is shown. (**A, C**) Quantification of colocalization using Image J software (n=10 cells, *p< 0.05), right

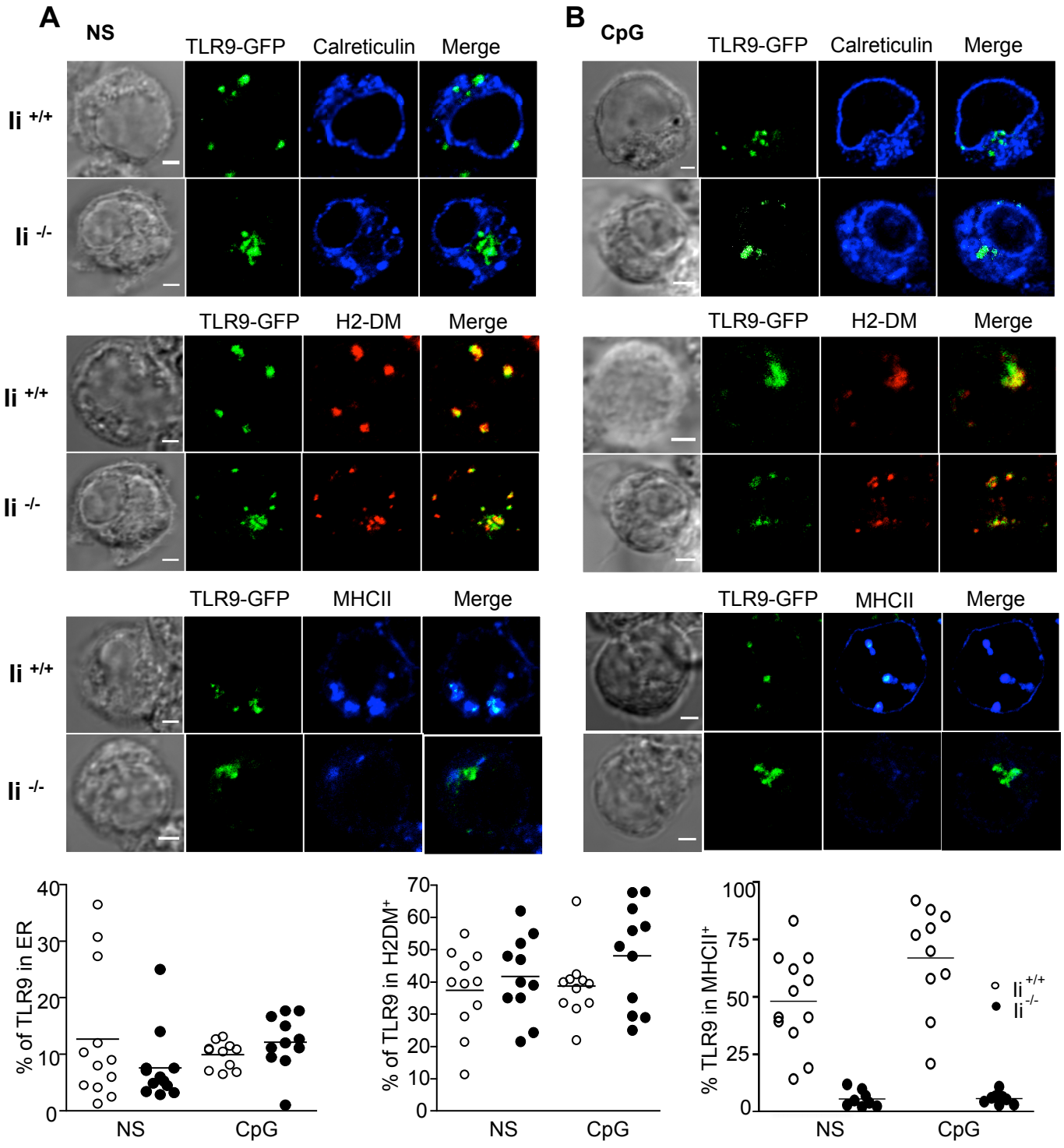

Fig S7. Ii does not regulate TLR9 trafficking in B cells. Immunofluorescence microscopy of resting (**A**) or TLR9-stimulated (**B**) $Ii^{+/+}$ or $Ii^{-/-}$ splenic B cells transfected with FL TLR9 tagged GFP and stained for TLR9 (green), calreticulin (blue), H2-DM (red) and MHCII (blue). One experiment representative out of three is shown. (**C**) Quantification of colocalization using Image J software (n=10), lower panel.

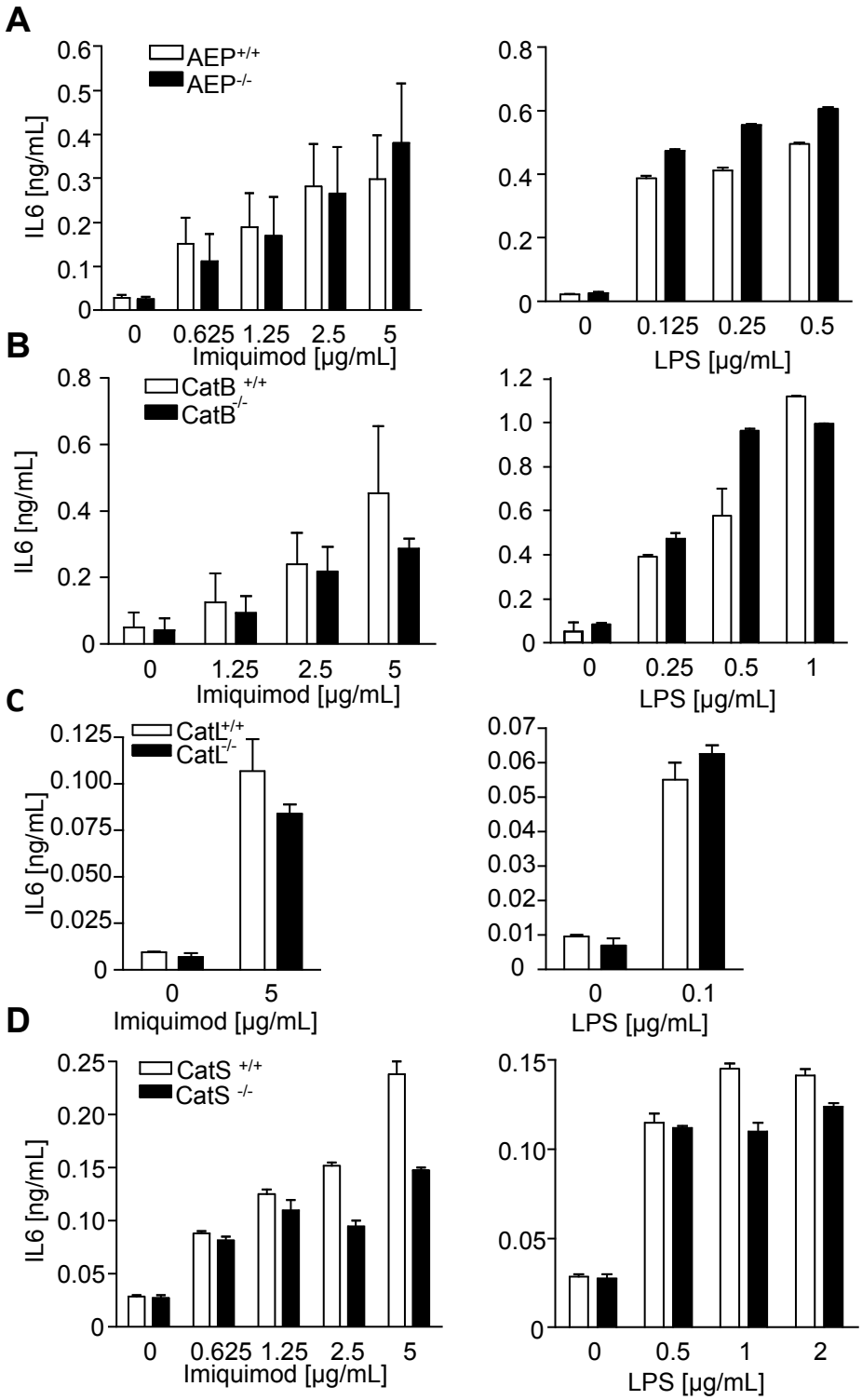

Fig S8. Cytokine production in wild type and different cysteine proteases deficient B cells upon TLR sensing. Wild type B cells or B cells deficient for AEP (**A**), cathepsin B (**B**), cathepsin L (**C**) and Cathepsin S (**D**) B cells were stimulated with imiquimod or LPS for 12h and secretion of IL-6 was measured by ELISA. (n=3, graphs show mean ± SEM).